Report 31: Estimating the burden of COVID-19 in Damascus, Syria: an analysis of novel data sources to infer mortality under-ascertainment

Oliver J. Watson,[1] Mervat Alhaffar,[2] Zaki Mehchy,[3] Charles Whittaker,[1] Zack Akil,[4] Imperial College COVID-19 Response Team,[1] Francesco Checchi,[2] Neil Ferguson,[1] Azra Ghani[1], Emma Beals,[5,6] Patrick Walker[1], Anonymous Authors*

[1]MRC Centre for Global Infectious Disease Analysis, Jameel Institute for Disease and Emergency Analytics, Imperial College London, London, UK
[2]Department of Infectious Disease Epidemiology, Faculty of Epidemiology and Population Health, London
[3]School of Hygiene and Tropical Medicine, London, UK
[4]Syria team, Conflict Research Programme, London Schools of Economics
[5]Google Cloud Developer Advocacy, Google, London, UK
[6]European Institute of Peace, Brussels, Belgium
[7]Middle East Institute, Washington, D.C.

Corresponding author: a.ghani@imperial.ac.uk

*Anonymous Author Acknowledgements:
We would also like to acknowledge the input of a dozen Syrian doctors, health officials, epidemiologists and academics who were instrumental in this analysis. They have significantly guided the study and should be considered as contributing authors but have requested to be acknowledged anonymously for security reasons.

Imperial College COVID-19 Response Team:
Kylie Ainslie, Marc Baguelin, Samir Bhatt, Adhiratha Boonyasiri, Olivia Boyd, Nicholas F Brazeau, Lorenzo Cattarino, Giovanni Charles, Constanze Ciavarella, Laura V Cooper, Helen Coupland, Zulma M Cucunuba, Gina Cuomo-Dannenburg, Bimandra A Djaafara, Christl A Donnelly, Ilaria Dorigatti, Oliver D Eales, Sabine L van Elsland, Fabricia F Nascimento, Richard G FitzJohn, Seth Flaxman, Alpha Forna,, Han Fu, Katy A M Gaythorpe, William D Green, Arran Hamlet, Katharina Hauck, David Haw, Sarah Hayes, Wes Hinsley, Natsuko Imai, Benjamin Jeffrey, Robert Johnson, David Jorgensen, Edward Knock, Daniel J Laydon, John A Lees, Thomas Mellan, Swapnil Mishra, Gemma Nedjati-Gilani, Pierre Nouvellet, Lucy C Okell, Daniela Olivera, Margarita Pons-Salort, Manon Ragonnet-Cronin, Igor Siveroni, Isaac Stopard, Hayley A Thompson, H Juliette T Unwin, Robert Verity, Michaela A C Vollmer, Erik Volz, Caroline E Walters, Haowei Wang, Yuanrong Wang, Lilith K Whittles, Peter Winskill, Xiaoyue Xi

DOI: https://doi.org/10.25561/82443

Summary

The COVID-19 pandemic has resulted in substantial mortality worldwide. However, to date, countries in the Middle East and Africa have reported substantially lower mortality rates than in Europe and the Americas. One hypothesis is that these countries have been 'spared', but another is that deaths have been under-ascertained (deaths that have been unreported due to any number of reasons, for instance due to limited testing capacity). However, the scale of under-ascertainment is difficult to assess with currently available data. In this analysis, we estimate the potential under-ascertainment of COVID-19 mortality in Damascus, Syria, where all-cause mortality data has been reported between 25th July and 1st August. We fit a mathematical model of COVID-19 transmission to reported COVID-19 deaths in Damascus since the beginning of the pandemic and compare the model-predicted deaths to reported excess deaths. Exploring a range of different assumptions about under-ascertainment, we estimate that only 1.25% of deaths (sensitivity range 1% - 3%) due to COVID-19 are reported in Damascus. Accounting for under-ascertainment also corroborates local reports of exceeded hospital bed capacity. To validate the epidemic dynamics inferred, we leverage community-uploaded obituary certificates as an alternative data source, which confirms extensive mortality under-ascertainment in Damascus between July and August. This level of under-ascertainment suggests that Damascus is at a much later stage in its epidemic than suggested by surveillance reports. We estimate that 4,340 (95% CI: 3,250 - 5,540) deaths due to COVID-19 in Damascus may have been missed as of 2nd September 2020. Given that Damascus is likely to have the most robust surveillance in Syria, these findings suggest that other regions of the country could have experienced similar or worse mortality rates due to COVID-19.

SUGGESTED CITATION

Oliver J. Watson, Mervat Alhaffar, Zaki Mehchy *et al.* Estimating the burden of COVID-19 in Damascus, Syria: an analysis of novel data sources to infer mortality under-ascertainment. Imperial College London (15-09-2020), doi: https://doi.org/10.25561/82443.

1. Introduction

The COVID-19 pandemic is a major global threat, with 25,327,098 cases and 848,255 deaths confirmed as of 1st September 2020 (*1*). The majority of countries have responded to the potential threat by implementing various non-pharmaceutical interventions, with many opting for society-wide suppression measures in an effort to prevent unacceptable loss of life (*2*). However, a number of low- and middle-income (LMICs) and/or conflict-affected countries in Africa and the Middle East, such as Tanzania, Sudan and Yemen have reported no sharp increase in mortality of the scale predicted by multiple modelling studies, even where interventions were limited (*3*, *4*). These observations are hard to reconcile with contemporaneous reports of hospitals becoming overwhelmed in these settings (*5*, *6*). They are also in contrast to reports from LMICs in Latin America that have witnessed major epidemics resulting in hundreds of thousands of deaths (*7*, *8*). Additionally, many of these settings with very low observed mortality are now reporting that cases and hospital bed demand are falling despite no notable change in implemented interventions or behaviour change (*9*). Consequently, many alternative explanations have been sought to understand the heterogeneity in the magnitude of COVID-19 epidemics seen across LMICs. These include exploring the effects of climate (*10*), population density (*11*), inter-pathogen effects (*12*), younger populations (*13*) and BCG vaccination (*14*) on COVID-19 transmission or clinical severity.

One alternative (or concurrent) explanation, which has garnered less attention within the scientific literature despite numerous reports in the media (*15*, *16*), is that COVID-19 related deaths have been substantially under-ascertained in some countries. Under-ascertainment of COVID-19 symptomatic cases has been recognised as an issue in many settings (both high and low income), due to factors such as limited testing capacity and the non-specific symptoms of mild disease [(17)]. Because clinically severe cases are more likely to be recognised and tested [(18)], mortality data have been viewed as a more reliable datastream for cross-country comparisons and for tracking epidemics [(19)]. However, under-ascertainment of COVID-19 deaths is known to occur, with investigations comparing excess mortality and reported lab-confirmed COVID-19 deaths revealing substantial discrepancies, particularly at the beginning of epidemics and at the peak of transmission (*16*, *20*). Consequently, all-cause, excess population mortality has been considered the most reliable data source for comparing the magnitude and trajectory of COVID-19 epidemics across countries (*21*). Unfortunately, real-time estimates of all-cause mortality are unavailable for many LMICs and conflict-affected countries where comprehensive vital registration systems are often lacking or data sharing is restricted (*22*).

DOI: https://doi.org/10.25561/82443

Motivated by reports of an overwhelmed health system (*23*) and widespread under-ascertainment of deaths (*24*) we sought to understand the evolving COVID-19 epidemic in Syria, a country that has been ravaged by war for nearly a decade. In particular, we focus on reports from the capital of Damascus, for which the governorate released a statement on 2nd August 2020 reporting the number of deaths recorded by the Damascus mortuary office between 25th July - 1st August (Supplementary Table 3) (*25*). During this 8-day period, 832 deaths were reported giving an average of 104 deaths per day. The reported deaths are significantly in excess of estimates of expected daily mortality, namely 32 deaths per day given annual mortality for Damascus reported by the Syrian Central Bureau of Statistics (CBS) (*26*). One week earlier, the director of the Damascus Burial of the Dead Office suggested that the pre-pandemic daily mortality in Damascus during this period of the year was "*approximately 40 deaths, a normal figure in the summer as deaths increase due to high heat*" (*27*). This estimate is in line with reports from 2016 by the same director that daily deaths are in the range of 15-50 deaths per day (*28*). Applying these broadly consistent pre-pandemic baselines, we computed approximate excess mortality, and in turn infer the level of under-ascertainment of COVID-19 deaths in Damascus.

2. Estimating the under-ascertainment of deaths

We extend a previously published (*3*) age-structured COVID-19 transmission model and fit the model to daily COVID-19 deaths reported in Damascus governorate (Supplementary Table 4). As of 2nd September 2020, 120 COVID-19 deaths had been reported in Syria, of which 60 were in Damascus governorate (Figure 1). During this time, a number of non-pharmaceutical interventions (NPI) were implemented in Damascus, including curfews, school and work closures and suspension of religious prayers, however most of these are reported to have been implemented prior to 11th May 2020 with many being relaxed on 26th May (Figure 1 and Supplementary Table 5). As in our previous work modelling healthcare burden in LMICs (*29*), we first estimate relative changes in individual-level mobility (and by extension, patterns of mixing and contact relevant to the transmission of respiratory viruses) over time. Specifically, we estimate mobility using a Boosted Regression Tree model (Supplementary Figure 1), trained to predict mobility patterns (as quantified in the Google Community Mobility Reports (*30*), which comprise 130 countries but are not available for Syria) based on government policies, as quantified by the ACAPs Government measures dataset (Supplementary Table 5) (*31*). We then estimate the effect of changes in mobility on SARS-CoV-2 transmission by fitting to the time series of daily COVID-19 deaths, allowing the effect size of mobility to differ after interventions are relaxed to reflect changes in human behaviour in response to COVID-19 (*32*).

DOI: https://doi.org/10.25561/82443

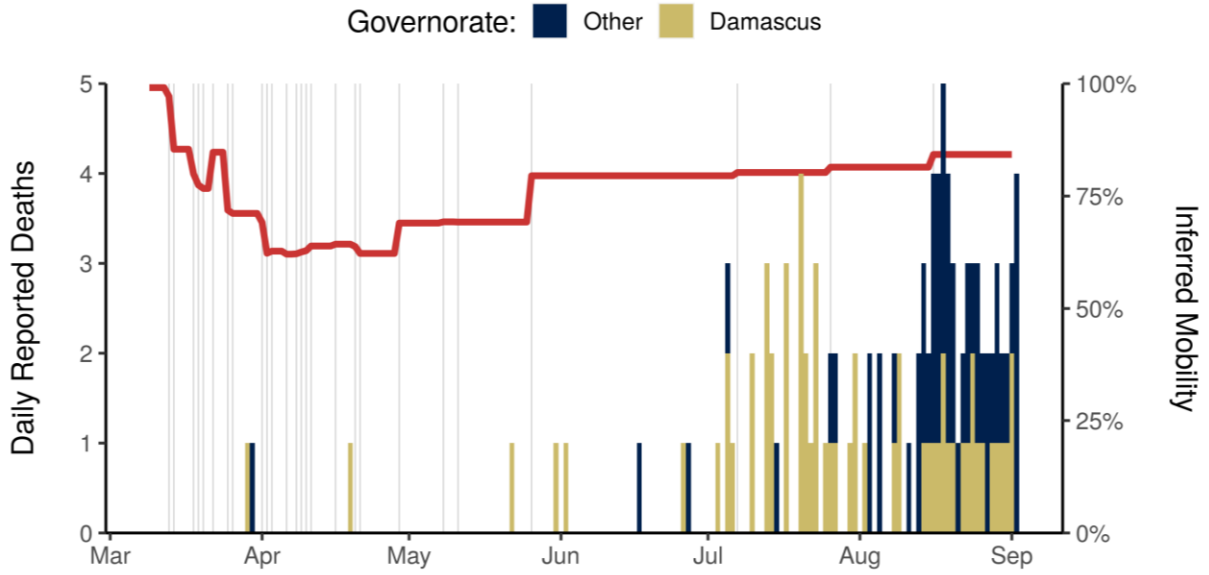

Figure 1. Incidence of confirmed deaths due to COVID-19 in Syria up to 2nd September 2020. Deaths reported by the Syrian Ministry of Health (*33*) are shown, with the deaths occurring in the Damascus governorate in gold. The inferred relative mobility pattern for Syria is superimposed with the red line (where 100% indicates the pre-epidemic baseline), with the timing of government interventions and policy changes indicated with grey vertical lines. As of 2nd September, 120 COVID-19 deaths had been reported in Syria, with 60 deaths in Damascus.

In order to estimate the level of under-ascertainment of deaths, we assume that a constant proportion of the model-predicted COVID-19 deaths on a given day are ascertained and reported. We scan across a range of under-ascertainment levels to relate the deaths predicted by the model to reported deaths. Reported deaths are assumed to follow a negative binomial distribution (to allow for observed over-dispersion of counts) with an expected mean value given by the model-predicted deaths multiplied by the level of under-ascertainment. If we assume a constant level of under-ascertainment, the trajectory of reported deaths should mirror the shape of the epidemic after accounting for under-ascertainment. Using this assumption we infer the level of under-ascertainment by comparing the model predicted deaths between 25th July - 1st August to the estimated excess mortality based on the government reported all-cause mortality data in Damascus for the same period.

Furthermore, our transmission model tracks the number of individuals predicted to develop symptoms sufficiently severe to require hospitalisation, either requiring oxygen support (in less severe cases) or mechanical ventilation (for those with the most severe symptoms). Some 204 intensive care unit (ICU) beds offer mechanical ventilation in Damascus across the private and public health system, with 47% estimated to be available for COVID-19 cases after accounting for expected occupancy due to non-COVID-19 health problems (*34*). We assume the number of hospital beds in functional hospitals is equivalent to the number of individuals who can be provided with oxygen support. The Health Resources and Services Availability Monitoring System (HeRAMS) estimated there were 3,245 hospital beds in functional hospitals in Damascus in 2020 (*35*). Using estimates of the proportion of beds in public health systems [(26)], we

estimate there are approximately 4,300 beds in functional hospitals in Damascus across both the private and public health systems. Based on inpatient data from previous years (*26*), we estimate that approximately 1935 (45%) of these beds are available for COVID-19 admissions after accounting for normal hospital demand. Based on UN estimates from the World Urbanization Prospects we assume a population size of 2,394,000 for Damascus governorate (*36*, *37*), with an age demographic identical to UN estimates for Syria (*36*). Given the extensive changes to Syrian demography and health services resulting from war, and ongoing uncertainty regarding key COVID-19 parameters, we conducted an extensive sensitivity analysis, exploring the impact that the assumed demography, population size in Damascus governorate, healthcare capacity, infection fatality ratios (IFRs) and baseline daily mortality have on the estimated level of under-ascertainment (Supplementary Table 6).

Adopting the default parameters, we estimate that 1 in 80 (1.25%) deaths due to COVID-19 have been reported in Damascus (Figure 2). This was determined by comparing the model-predicted deaths between 25th July - 1st August to the excess mortality under the assumption that all excess deaths are due to COVID-19 (Figure 2a). If we double our assumed baseline death rate from 32 to 64 deaths per day, we still estimate substantial under-ascertainment with an estimated 1 in 50 deaths due to COVID-19 being reported as such (Figure 2b). To explore the reliability of these model fits, we also looked at reports of when hospitals were reported to be at capacity in Damascus. These reports vary, but there is consensus that individuals were reluctant to go to hospitals sometime between 17th July (*38*) and 30th July (*39*) due to hospital reaching capacity and having to turn away patients. With our default parameters, we predict that hospital capacity would have been reached during this period with an assumed under-ascertainment of deaths between 1% and 1.25% (Figure 2c). This lends further support to our inferred most likely under-ascertainment of 1.25%. This finding is dependent on the assumed number of hospital beds available. However, in our sensitivity analysis the best model fit to mortality data was obtained assuming approximately 2,000 hospital beds were available, consistent with the value of 1,935 beds used to generate our central estimates (Supplementary Figure 2). Sensitivity analysis showed our estimates to be robust to varying assumptions about the population size and demography of the Damascus population. However, we obtained a better model fit when we assumed a higher IFR than given by the Verity et al. estimates (*40*). Higher IFRs are plausible if access to oxygen support was limited at the peak of the epidemic (*3*). Looking across the full range of assumptions examined in the sensitivity analysis, we estimate that between 1% and 3% of deaths due to COVID-19 were ascertained and reported.

DOI: https://doi.org/10.25561/82443

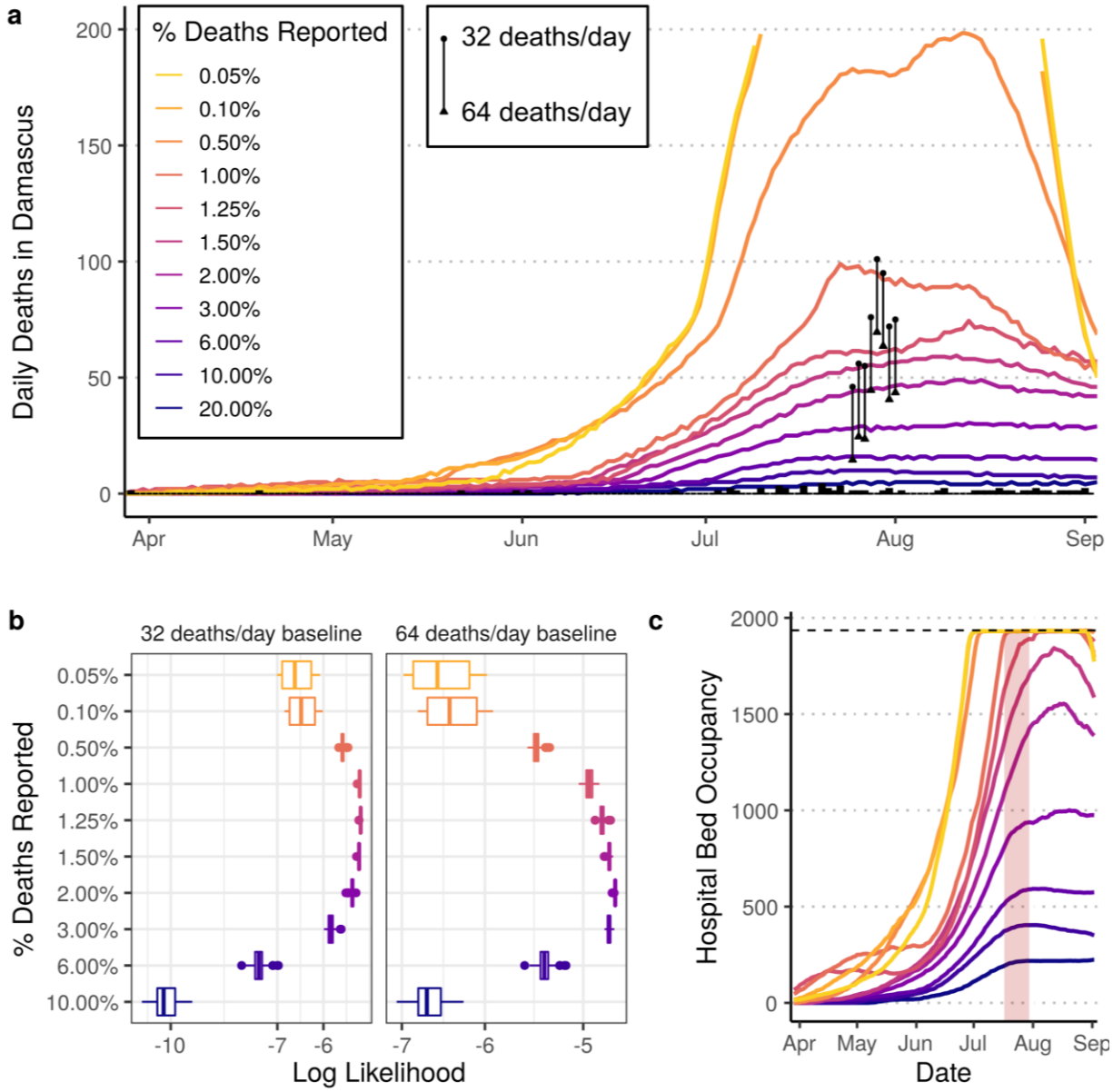

Figure 2. Estimates of under-ascertainment of deaths in Damascus. In a) the daily model-predicted deaths in Damascus are shown using the default model parameters and a range of values for the under-ascertainment of COVID-19 deaths. Excess deaths for an 8-day period are shown with point ranges, with estimates assuming a baseline of 32 and 64 deaths per day shown with a circle and triangle respectively. In b) the log likelihood for each level of under-ascertainment is shown for different assumed baseline mortality. Model log likelihoods presented reflect the mean model log likelihood across the full sensitivity analysis conducted, suggesting that under-ascertainment is likely between 1% - 3% when viewed across both baseline mortality estimates. In c) the model-predicted hospital occupancy for the simulations in a) are shown. The hospital capacity for Damascus is shown with a dashed horizontal line, with the 2-week period in which hospitals were reported to be first at capacity shown shaded in red.

DOI: https://doi.org/10.25561/82443

3. Implications of under-ascertainment for the Damascus epidemic

The scale of inferred under-ascertainment indicates a starkly different epidemic from that suggested by reported deaths, with implications for its future trajectory To reconstruct the course of the epidemic to date and forecast its future trajectory, we selected the best-fitting model from the default parameter set, which assumed that 1.25% of COVID-19 deaths are reported, and projected it forward for 120 days, assuming that the interventions and population contact patterns remain constant after 2nd September 2020. We estimate that 4,440 (95% CI: 3,310 - 5,60) deaths have occurred in Damascus up to 2nd September 2020 (Figure 3a). We estimate that there were 67,290 (95% CI: 44,610 - 77,910) active infections in Damascus on 2nd September 2020, with 9,760 (95% CI: 6,470 - 11,360) newly infected individuals, including both asymptomatic and symptomatic infections. Consequently, we predict that a cumulative total of 39.0% (95% CI: 32.5% - 45.0%) of the population in Damascus had been infected by 2nd September 2020 (Figure 3d). Assuming that the current level of interventions remains in place, we predict that the epidemic has passed its peak in transmission. We estimate that 240 (95% CI: 170 - 280) new COVID-19 cases requiring hospital level health interventions occurred on 2nd September 2020, with the peak in hospitalisation requirement predicted to have occurred one month earlier during the 1st week of August 2020. However, despite the decrease in admissions, we predict that there have been insufficient hospital beds for the majority of August 2020, with beds becoming available again from the 28th August 2020 (Figure 3c).

We predict that the early indicators of declines in transmission observed in Damascus will continue, with 49.1% (95% CI: 41.7% - 54.7%) of the population being infected by the end of 2020. The recent decline in transmission in Damascus is largely due to increasing immunity in the population and the resultant depletion of susceptible individuals (Supplementary Figure 3). We estimate that the effective reproduction number, R_{eff}, for Damascus was 0.87 (95% CI: 0.82 - 0.92) on 2nd September 2020. In the absence of immunity, we estimate that R_t, namely the reproduction number unadjusted for population immunity, would have been 1.48 (95% CI: 1.34 - 1.65) on 2nd September 2020. This is significantly lower than the estimate of R_0, which was estimated to be 2.77 (95% CI: 2.45 - 2.94), which given the majority of interventions in Damascus have now been relaxed, suggests that individual-level behavioural changes have led to a reduction in transmission since the beginning of the epidemic.

DOI: https://doi.org/10.25561/82443

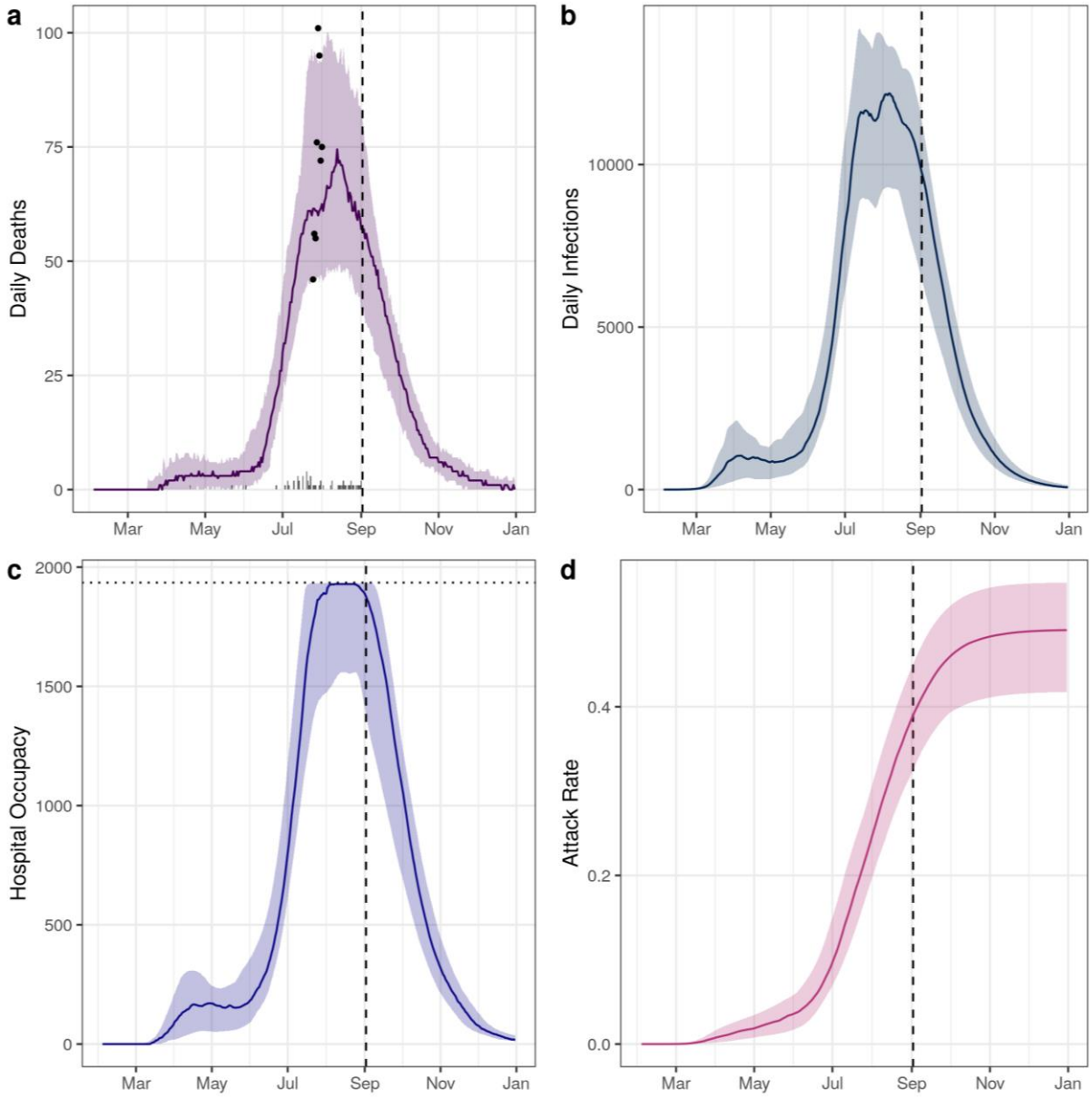

Figure 3. Model-predicted deaths, infections, hospital occupancy and attack rates of COVID-19 for Damascus. The best-fitting model to excess deaths (assumed baseline mortality as 32 deaths per day) is shown, which estimates that 1.25% of deaths are reported. In a) and b) the reported daily deaths and infections due to COVID-19 respectively are shown, with the estimated excess deaths for a baseline mortality of 32 deaths per day shown in a) as points. In c) hospital occupancy over time is shown, with the dotted horizontal line showing the hospital capacity available. In d) the attack rate in Damascus is shown. In all plots, the confidence interval represents the 95% quantile range and a vertical dashed line is shown for 2nd September 2020 when the analysis was conducted. The 4-month projection assuming the current level of transmission is shown in each plot.

DOI: https://doi.org/10.25561/82443

4. Alternative epidemic trajectories

The excess mortality recorded between 25th July - 1st August provides a small window to analyse the COVID-19 epidemic in Damascus. However, there are multiple possible epidemic trajectories that could yield the number of excess deaths reported. In Supplementary Figure 7, we explore three alternative scenarios and their compatibility with the observed data. One of these (Supplementary Figure 7D) is, like our default scenario, compatible with all the data streams analysed, namely reported daily deaths, excess deaths and the timing of the health system reaching capacity. It differs from the default scenario in assuming that only COVID-19 deaths occurring in hospitals are reported, with all deaths outside of hospitals (due to no available beds) assumed to be unreported. Additionally, it assumes that officially reported COVID-19 deaths prior to the 26th June are not linked to the current epidemic. This assumption is introduced as the last reported death prior to 26th June occurred 24 days earlier, which is greater than our assumed time from infection to death (*3*), suggesting that the current epidemic was seeded by recent importation events.

With these alternative assumptions, we again predict significant under-ascertainment, with the best-fitting model suggesting 3% of deaths occurring in hospitals are reported (Figure 4). This level of under-ascertainment yielded a good agreement with the three sources of data that we have been evaluating against: reported deaths (Figure 4a), excess deaths (Figure 4b) and the timing at which hospital capacity is reached (Figure 4c). The higher ascertainment predicted in this scenario compared to our original analysis estimate of 1.25% reflects a plateau in reported deaths when health services are beyond capacity. Consequently, the proportion of deaths reported will fall sharply when the health system reaches capacity. Overall, we estimate that 0.28% (95% CI: 0.24% - 0.39%) of total COVID-19 deaths are reported in this scenario. The resultant epidemic trajectory predicts a significantly larger number of excess deaths compared to the original analysis, with 21,255 deaths (95% CI: 15,358 - 24,857) estimated by 2nd September 2020 and an attack rate of 83.7% (95% CI: 79.9% - 87.4%) by the end of 2020 (Supplementary Figure 8).

The substantial differences in these trajectories reflect both the difficulties in only having 8 days of excess mortality to characterise the extent of the COVID-19 epidemic in Damascus, and relying on the assumption that a constant relationship exists between the reported deaths and excess mortality. However, there are many reasons why this relationship may be more complex than this, such as changing testing capacity over time (Supplementary Figure 6) and altered treatment-seeking behaviour in response to reports of limited hospital beds (*38*). Given these difficulties, we sought to gain an alternative source of data for mortality trends in Damascus.

DOI: https://doi.org/10.25561/82443

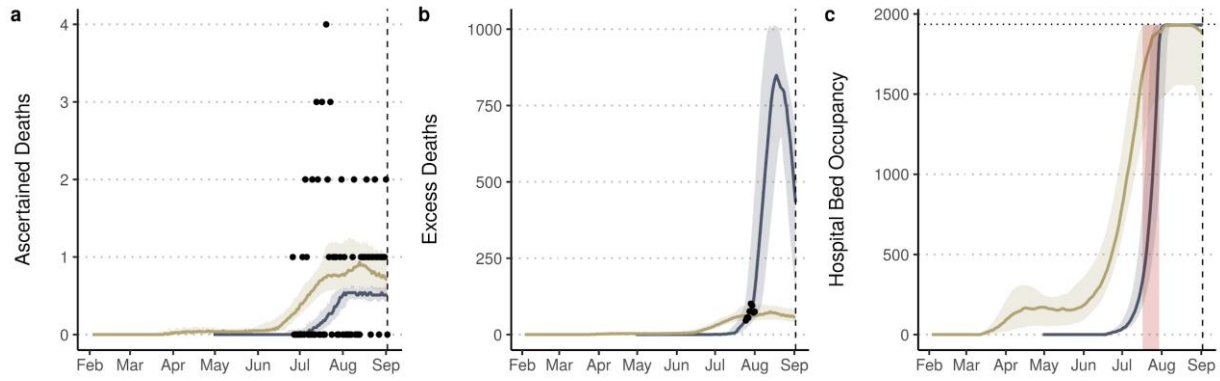

Figure 4. Alternative epidemic trajectories for Damascus. The best-fitting model for the default parameters is shown under the assumption that a fixed proportion of all deaths are reported (gold) and also under the assumption under that only deaths within the health system may be reported (blue). The model-predicted a) ascertained deaths, b) excess deaths and c) hospital bed occupancy are shown for both epidemic trajectories. In c) the hospital capacity for Damascus is shown with a dashed horizontal line, with the 2-week period in which hospitals were reported to be first at capacity shown shaded in red.

5. Estimating excess mortality in Damascus from obituary certificates

Traditionally, when individuals die in Damascus, a paper certificate of death is printed and affixed to household walls in nearby neighbourhoods of the deceased. These certificates include information, such as the date of death, details of the deceased's relatives and the consolation events being held. However, due to internal displacements and a high number of Syrians leaving the country due to recent conflict, a community maintained Facebook page ("Damascus Mortality" (*41*)) was established, where images of the certificates are routinely uploaded in order to inform people about deaths in Damascus. Despite the informality of this process, the observed mortality trends in this alternative data source reveal a consistent baseline of 300 certificates per month in 2017 - 2019 (Figure 5a). By contrast, uploaded certificates rose to 809 in July and 1066 in August 2020, with a clear peak at the end of July (Figure 5b).

To obtain an additional view of the epidemic in Damascus, we separately fitted our transmission model to the certificate data source. We calculated the excess certificate deaths for 2020 by subtracting the mean number of certificates uploaded daily in 2017 - 2019 for each month from those reported in 2020 (Figure 5c). The inferred estimates suggest that excess deaths increased from the beginning of July, aligning with our previous assumption introduced in Figure 4. We therefore fitted the model to excess death certificates from July onwards, assuming that the current epidemic is the result of recent importation events. Given the uncertainty in the fraction of total COVID-19 deaths the excess death certificates represent, we used three approaches when fitting to death certificates. Firstly, we use a similar approach to when fitting daily reported deaths, in which we identify the ascertainment fraction (here referring to the proportion of total COVID-19 deaths that are reported in the excess deaths certificates) that best fits the 8-day government reported excess mortality. We also explore a maximum upper and

DOI: https://doi.org/10.25561/82443

lower ascertainment fraction, either assuming that 100% of COVID-19 deaths are captured by the excess death certificates or that only 27.5% of COVID-19 deaths are captured by the certificates, which reflects the proportion of total all-cause mortality in Damascus that was captured by the certificates in 2017-2019 (*26*).

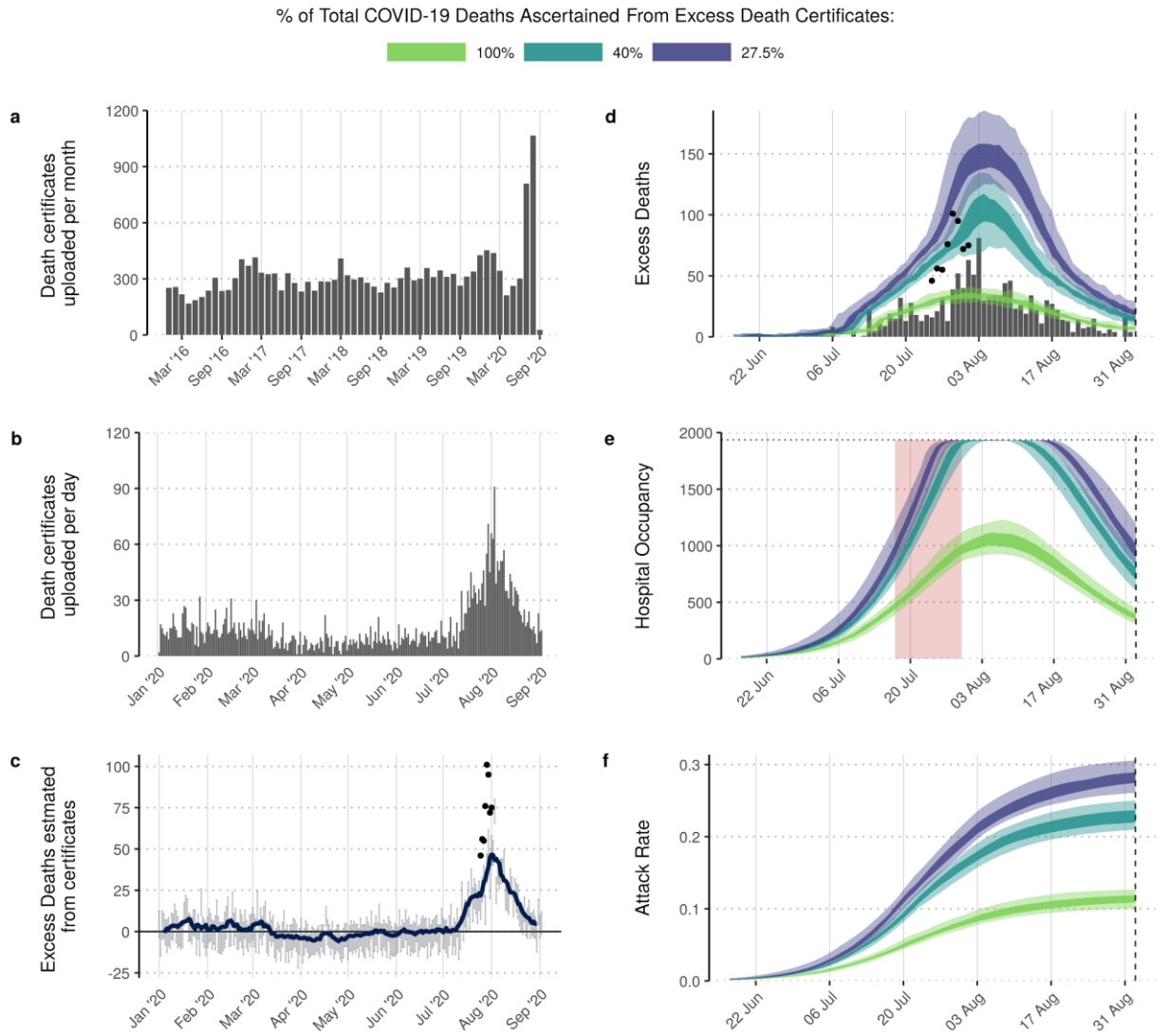

Figure 5. Community-uploaded death certificates in Damascus and the inferred epidemic trajectory. In a) we show the number of obituary certificate photos uploaded monthly to the community maintained "Damascus Mortality" Facebook page, with the daily uploads in 2020 in b) revealing a significant increase in July and August 2020. In c), the inferred excess death certificates are shown, with error bars showing the 95% CI and the blue line indicating the weekly average excess deaths. In d) model fits to the certificate excess death data (vertical bars) are shown under different assumptions of the proportion of total COVID-19 deaths that are ascertained by the excess death certificates. In both c) and d) the points show the government-reported excess deaths between 25th July - 1st August. The predicted hospital occupancy is shown in e), with the hospital capacity for Damascus shown with a dashed horizontal line, with the 2-week period in which hospitals were reported to be first at capacity shown shaded in red. In f) the inferred attack rate is shown up to 2nd September 2020. In d), e) and f), both the 50% CI and 95% CI are presented with dark and light shading respectively.

Comparing the best-fitting model to the reported government excess deaths, we estimate that the excess death certificates represent 40% of the total COVID-19 deaths (Figure 5d). Using this model, we estimate 2,920 COVID-19 deaths (95% CI: 2,480 - 3,460) by 2nd September 2020, which amounts to 2% of COVID-19 deaths in Damascus being reported. Using the upper (100%) and lower (27.5%) assumed percentage of total COVID-19 deaths captured by the death certificate data, we estimate that 1.5% - 5% of deaths since July were reported. The upper estimate, however, is unlikely to be reflective of the situation in Damascus, with estimated hospital bed occupancy never exceeding capacity as reported at the end of July (Figure 5e). The lower estimate, by contrast, is close to our default best-fitting model in Figure 3, in which we estimate that 3,820 COVID-19 deaths (95% CI: 2,800 - 4,800) occurred between 1st July - 2nd September 2020, comparable to the estimated 4,200 COVID-19 deaths (95% CI: 3,710 - 5,000) made when assuming that excess death certificates represent 27.5% of the total COVID-19 deaths.

The excess death certificate data provide supporting evidence that the recent decline in transmission predicted by the default model has indeed occurred in Damascus. However, the decline in excess death certificates started earlier than the predictions of the default model. With the best-fitting model to excess death certificates, we estimate that hospital beds became available again from approximately the 16th August 2020 (Figure 5b). The shorter epidemic observed also leads to a lower estimated attack rate by 2nd September (Figure 5c). Using the best-fitting model (40% of COVID-19 deaths captured by certificates) we estimate that 22.8% (95% CI: 21.0% - 25.0%) of the population were infected between 1st July and 2nd September, whilst the lower estimate of 27.5% of COVID-19 deaths captured by certificates estimates an attack rate of 28.0% (95% CI: 26.1% - 30.6%). This latter estimate is similar to the 29.3% (95% CI: 23.1% - 32.5%) estimated during the same period using the default model.

DOI: https://doi.org/10.25561/82443

6. Discussion

The apparent absence of high levels of mortality in Syria given the extent of transmission occurring elsewhere in the region is surprising given the ubiquitous nature of transmission of a new pathogen that was expected and borne-out in many other regions of the world. Based on reports of all-cause mortality released from the governorate of Damascus over the period 25th July - 1st August, we conclude that the reported COVID-19 deaths only capture a small proportion of the true number of deaths due to COVID-19 in that city. Despite the estimate of excess mortality only being available for just over a week, we estimate that 1.25% (sensitivity range 1% - 3%) of deaths from COVID-19 have been reported in Damascus. As a consequence, it is likely that the epidemic in Damascus is in a much more advanced stage than the reported data would suggest, with approximately 40% of the population already infected.

Despite the predicted downwards trajectory of the epidemic there is still need for the reductions in transmission achieved by behavioural changes to be maintained. It seems unlikely that any country will see transmission return to initial R_0 values due to the level of COVID-19 awareness that people have compared to the beginning of 2020 (*42*). However, if human behaviour towards COVID-19 relaxes, it remains possible that transmission would increase within Damascus, despite the high attack rates we estimate have occurred thus far. Assuming that the reproduction number in the absence of immunity increased from our estimate of 1.48 to 2.0, approximately equal to our estimate of R_t a week after the first government intervention in Syria (Supplementary Figure 3), current declines in transmission could be reversed (Supplementary Figure 4). Under this scenario, we predict that the death rate due to COVID-19 will not surpass its previous peak, but the demand for hospital level health interventions will continue to exceed capacity until the beginning of October. This would likely have significant secondary impacts on overall mortality in Damascus. One such impact would be the continued toll on medical personnel who have been reported to have been heavily affected by the epidemic, with reports of at least 60 Syrian doctors, mostly in Damascus, dying from COVID-19 by 18th August 2020 (*43*). High levels of healthcare worker infection and mortality would likely further decrease the capacity to effectively treat COVID-19 patients, which are already stretched in Syria, with a UN report dated 6th March 2020 stating that up to 70% of health workers had left Syria as migrants or refugees or been killed during the conflict (*44*).

We have only been able to gain an insight into the situation in Damascus due to the publication of mortality data from Damascus by the governorate on 2nd August for the previous 8 days. This approach relies on a reliable estimate of baseline mortality, which were sourced from previous annual mortality estimates. However, there are undoubtedly indirect effects that COVID-19 places on healthcare systems, which are hard to quantify but are widely expected to increase all-cause mortality (*45*). However, even when we doubled our baseline (non COVID-19) mortality assumption, we still estimate considerable under-ascertainment of COVID-19 deaths, with a maximum of 3% of such deaths being reported. Another assumption was our use of age-stratified infection fatality ratios taken from Verity et al (*40*), which were derived from Chinese data very early in the pandemic and therefore assume a standard of healthcare comparable to that available in China. We explored in our sensitivity analysis this assumption and introduced scenarios in which poorer health outcomes occurred, e.g. due to insufficient oxygen provision. This did not change the inferred level of death under-ascertainment, but does lead to lower estimated

DOI: https://doi.org/10.25561/82443

cumulative attack rates to date (Supplementary Figure 5). Given that 8% of functional public hospitals lacked oxygen support (*46*) it is likely that the default parameter estimate of attack rates of 39.0% is an upper estimate, and the true value likely exists between this estimate and the estimate of 30.0% (95% CI: 24.9% - 34.3%) that we obtained assuming poorer health outcomes. However, a lower attack rate will mean that if transmission increases in the future due to increasing contact rates in the population, firm interventions in Damascus will need to be introduced to prevent a substantial second wave of infection. Central to this is an urgent need for testing to be increased, with only 18,238 COVID-19 tests conducted in Damascus as of 10th August 2020 (Supplementary Figure 6).

In our approach we rely on the assumption that mortality under-ascertainment is both constant over time and sufficient to relate reported daily deaths to excess mortality. However, we have acknowledged that this assumption may not be accurate, which in combination with relying only on 8 days of excess mortality data makes it impossible to be confident in the shape of the epidemic. For example, in Figure 4 we demonstrated how an unmitigated epidemic leading to 80% attack rates could explain the official reported data equally well if we assume that deaths are only reported for people who die in hospitals. The absence of consistent, reliable estimates of excess mortality is not unique to Damascus and as such alternative data sources are likely to be needed in many settings to understand how widespread COVID-19 may be. In this study, we also leveraged community-uploaded death certificates, demonstrating the benefit gained from this additional perspective of the epidemic in Damascus. Viewed together with reported excess mortality, they provide a consistent picture of a much higher level of mortality and a more mature epidemic than official data would suggest. The precise size of that epidemic, however, is uncertain and is affected by our assumptions about how accurately the death certificates reflect all cause mortality in Damascus. The consistent trends in mortality prior to 2020 lead us to believe that this data source is very useful, yet still likely to be subject to changing biases over time, in particular during the pandemic. For example, more death certificates than normal may be uploaded with individuals concerned that individuals will be less likely to read the affixed obituary notices in person due to fears of the spread of COVID-19. Alternatively, the certificates may continue to capture the same percentage (27.5%) of all-cause mortality as they did in 2017 - 2019. If this is the case, it would suggest that the reported excess deaths between 25th July - 1st August underestimate total COVID-19 deaths during this period.

The analysis presented here was only possible because the Damascus governorate office published mortality data at a key time in the Damascus epidemic. Although this was only 8 days of data, the epidemic trajectory after these dates aligns with a plateauing in the reported COVID-19 deaths in Damascus after 2nd August. Further support for a decline in the epidemic is suggested by changes in community-uploaded obituary certificates to Facebook from August onwards. However, during this time a notable rise in reported cases and deaths was observed in other governorates of Syria. This could signal large epidemics becoming visible outside Damascus, a pattern which has been observed across many other countries (*47*). Alternatively, increases in testing capacity could mean that each governorate is at an earlier point in their epidemic compared to Damascus for the same number of deaths (*23*), with epidemics being seeded by Damascus when inter-governorate travel bans were lifted. Neither hypothesis can be explored effectively without a more reliable data source on mortality. While the level of under-ascertainment across Syria may be similar to that in Damascus, this seems unlikely given the heterogeneity in health infrastructure and

testing resources. This need for more reliable and regular data streams for measuring mortality, and for government transparency in publishing available data, is equally pressing for many low- and middle-income countries and conflict affected settings. However, in the absence of such data, alternative data sources will have to be leveraged in order to characterise the dynamics of COVID-19 in many parts of the world. Our analysis provides one example of the level of data that must be included if we are to understand the extent to which the COVID-19 pandemic may have occurred unobserved to date in much of the world.

7. Acknowledgements

We would like to thank a Wikipedia user - RamiPat (https://en.wikipedia.org/wiki/User:RamiPat), who has updated the Syria COVID-19 wikipedia page daily, copying the reported deaths and cases from the Syrian MoH dashboard, which enabled us to identify the date of 1 death outside of Damascus that was not reported in the published daily COVID-19 reports. We would also like to thank Syria in Context with support from Heinrich Boell Stiftung for providing initial reporting on the excess death data. We would also like to thank Rim Turkmani and Mazen Gharibah from the Syria team at the Conflict Research Programme at London Schools of Economics. This work was supported by funding from The Wellcome Trust under a concordat agreement with the UK Foreign, Commonwealth and Development Office. We additionally acknowledge support from the UK Medical Research Council as well as Google for credits used during image processing of death certificate data.

8. References

1. WHO Coronavirus Disease (COVID-19) Dashboard, (available at https://covid19.who.int/).

2. N. G. Davies, A. J. Kucharski, R. M. Eggo, A. Gimma, W. J. Edmunds, Centre for the Mathematical Modelling of Infectious Diseases COVID-19 working group, Effects of non-pharmaceutical interventions on COVID-19 cases, deaths, and demand for hospital services in the UK: a modelling study. *Lancet Public Health*. **5**, e375–e385 (2020).

3. P. G. T. Walker, C. Whittaker, O. J. Watson, M. Baguelin, P. Winskill, A. Hamlet, B. A. Djafaara, Z. Cucunubá, D. Olivera Mesa, W. Green, H. Thompson, S. Nayagam, K. E. C. Ainslie, S. Bhatia, S. Bhatt, A. Boonyasiri, O. Boyd, N. F. Brazeau, L. Cattarino, G. Cuomo-Dannenburg, A. Dighe, C. A. Donnelly, I. Dorigatti, S. L. van Elsland, R. FitzJohn, H. Fu, K. A. M. Gaythorpe, L. Geidelberg, N. Grassly, D. Haw, S. Hayes, W. Hinsley, N. Imai, D. Jorgensen, E. Knock, D. Laydon, S. Mishra, G. Nedjati-Gilani, L. C. Okell, H. J. Unwin, R. Verity, M. Vollmer, C. E. Walters, H. Wang, Y. Wang, X. Xi, D. G. Lalloo, N. M. Ferguson, A. C. Ghani, The impact of COVID-19 and strategies for mitigation and suppression in low- and middle-income countries. *Science*. **369**, 413–422 (2020).

4. K. van Zandvoort, C. I. Jarvis, C. Pearson, N. G. Davies, CMMID COVID-19 working group, T. W. Russell, A. J. Kucharski, M. J. Jit, S. Flasche, R. M. Eggo, F. Checchi, Response strategies for COVID-19 epidemics in African settings: a mathematical modelling study. *medRxiv* (2020), , doi:10.1101/2020.04.27.20081711.

5. Yemen: “COVID-19 has made the health system’s collapse complete” (2020), (available at https://www.msf.org.uk/article/yemen-%E2%80%9Ccovid-19-has-made-health-systems-collapse-complete%E2%80%9D).

6. Health Alert: U.S. Embassy Dar es Salaam (2020), (available at https://tz.usembassy.gov/health-alert-u-s-embassy-dar-es-salaam-may-13-2020/).

7. D. S. Candido, I. M. Claro, J. G. de Jesus, W. M. Souza, F. R. R. Moreira, S. Dellicour, T. A. Mellan, L. du Plessis, R. H. M. Pereira, F. C. S. Sales, E. R. Manuli, J. Thézé, L. Almeida, M. T. Menezes, C. M. Voloch, M. J. Fumagalli, T. M. Coletti, C. A. M. da Silva, M. S. Ramundo, M. R. Amorim, H. H. Hoeltgebaum, S. Mishra, M. S. Gill, L. M. Carvalho, L. F. Buss, C. A. Prete Jr, J. Ashworth, H. I. Nakaya, P. S. Peixoto, O. J. Brady, S. M. Nicholls, A. Tanuri, Á. D. Rossi, C. K. V. Braga, A. L. Gerber, A. P. de C Guimarães, N. Gaburo Jr, C. S. Alencar, A. C. S. Ferreira, C. X. Lima, J. E. Levi, C. Granato, G. M. Ferreira, R. S. Francisco Jr, F. Granja, M. T. Garcia, M. L. Moretti, M. W. Perroud Jr, T. M. P. P. Castiñeiras, C. S. Lazari, S. C. Hill, A. A. de Souza Santos, C. L. Simeoni, J. Forato, A. C. Sposito, A. Z. Schreiber, M. N. N. Santos, C. Z. de Sá, R. P. Souza, L. C. Resende-Moreira, M. M. Teixeira, J. Hubner, P. A. F. Leme, R. G. Moreira, M. L. Nogueira, Brazil-UK Centre for Arbovirus Discovery, Diagnosis, Genomics and Epidemiology (CADDE) Genomic Network, N. M. Ferguson, S. F. Costa, J. L. Proenca-Modena, A. T. R. Vasconcelos, S. Bhatt, P. Lemey, C.-H. Wu, A. Rambaut, N. J. Loman, R. S. Aguiar, O. G. Pybus, E. C. Sabino, N. R. Faria, Evolution and epidemic spread of SARS-CoV-2 in Brazil. *Science* (2020), doi:10.1126/science.abd2161.

8. T. Burki, COVID-19 in Latin America. *Lancet Infect. Dis.* **20**, 547–548 (2020).

9. Yemen COVID-19 report. 2020-08-17 (2020), (available at https://mrc-ide.github.io/global-lmic-reports/YEM/).

10. C. J. Carlson, J. D. Chipperfield, B. M. Benito, R. J. Telford, R. B. O'Hara, Don't gamble the COVID-19 response on ecological hypotheses. *Nat Ecol Evol* (2020), doi:10.1038/s41559-020-1279-2.

11. J. Rocklöv, H. Sjödin, High population densities catalyse the spread of COVID-19. *J. Travel Med.* **27** (2020), doi:10.1093/jtm/taaa038.

12. M. Mbow, B. Lell, S. P. Jochems, B. Cisse, S. Mboup, B. G. Dewals, A. Jaye, A. Dieye, M. Yazdanbakhsh, COVID-19 in Africa: Dampening the storm? *Science*. **369**, 624–626 (2020).

13. N. G. Davies, P. Klepac, Y. Liu, K. Prem, M. Jit, CMMID COVID-19 working group, R. M. Eggo, Age-dependent effects in the transmission and control of COVID-19 epidemics. *Nat. Med.* **26**, 1205–1211 (2020).

14. L. E. Escobar, A. Molina-Cruz, C. Barillas-Mury, BCG vaccine protection from severe coronavirus disease 2019 (COVID-19). *Proc. Natl. Acad. Sci. U. S. A.* **117**, 17720–17726 (2020).

15. J. S. Stephanie Findlay, Delhi accused of under-reporting coronavirus deaths. *Financial Times* (2020), (available at https://www.ft.com/content/5049c66f-449d-4a13-ba1c-f95893b60597).

16. J. Wu, A. McCann, J. Katz, E. Peltier, 161,000 Missing Deaths: Tracking the True Toll of the Coronavirus Outbreak. *The New York Times* (2020), (available at https://www.nytimes.com/interactive/2020/04/21/world/coronavirus-missing-deaths.html).

17. L. Wynants, B. Van Calster, G. S. Collins, R. D. Riley, G. Heinze, E. Schuit, M. M. J. Bonten, J. A. A. Damen, T. P. A. Debray, M. De Vos, P. Dhiman, M. C. Haller, M. O. Harhay, L. Henckaerts, N. Kreuzberger, A. Lohman, K. Luijken, J. Ma, C. L. Andaur, J. B. Reitsma, J. C. Sergeant, C. Shi, N. Skoetz, L. J. M. Smits, K. I. E. Snell, M. Sperrin, R. Spijker, E. W. Steyerberg, T. Takada, S. M. J. van Kuijk, F. S. van Royen, C. Wallisch, L. Hooft, K. G. M. Moons, M. van Smeden, Prediction models for diagnosis and prognosis of covid-19 infection: systematic review and critical appraisal. *BMJ*. **369**, m1328 (2020).

18. E. Lavezzo, E. Franchin, C. Ciavarella, G. Cuomo-Dannenburg, L. Barzon, C. Del Vecchio, L. Rossi, R. Manganelli, A. Loregian, N. Navarin, D. Abate, M. Sciro, S. Merigliano, E. De Canale, M. C. Vanuzzo, V. Besutti, F. Saluzzo, F. Onelia, M. Pacenti, S. G. Parisi, G. Carretta, D. Donato, L. Flor, S. Cocchio, G. Masi, A. Sperduti, L. Cattarino, R. Salvador, M. Nicoletti, F. Caldart, G. Castelli, E. Nieddu, B. Labella, L. Fava, M. Drigo, K. A. M. Gaythorpe, Imperial College COVID-19 Response Team, A. R. Brazzale, S. Toppo, M. Trevisan, V. Baldo, C. A. Donnelly, N. M. Ferguson, I. Dorigatti, A. Crisanti, Suppression of a SARS-CoV-2 outbreak in the Italian municipality of Vo'. *Nature*. **584**, 425–429 (2020).

19. S. Flaxman, S. Mishra, A. Gandy, H. J. T. Unwin, T. A. Mellan, H. Coupland, C. Whittaker, H. Zhu, T. Berah, J. W. Eaton, M. Monod, Imperial College COVID-19 Response Team, A. C. Ghani, C. A. Donnelly, S. Riley, M. A. C. Vollmer, N. M. Ferguson, L. C. Okell, S. Bhatt, Estimating the effects of non-pharmaceutical interventions on COVID-19 in Europe. *Nature*. **584**, 257–261 (2020).

20. L. S. Vestergaard, J. Nielsen, L. Richter, D. Schmid, N. Bustos, T. Braeye, G. Denissov, T. Veideman, O. Luomala, T. Möttönen, A. Fouillet, C. Caserio-Schönemann, M. An der Heiden, H. Uphoff, T. Lytras, K. Gkolfinopoulou, A. Paldy, L. Domegan, J. O'Donnell, F. De' Donato, F. Noccioli, P. Hoffmann, T. Velez, K. England, L. van Asten, R. A. White, R. Tønnessen, S. P. da Silva, A. P. Rodrigues, A. Larrauri, C. Delgado-Sanz, A. Farah, I. Galanis, C. Junker, D. Perisa, M. Sinnathamby, N. Andrews, M. O'Doherty, D. F. Marquess, S. Kennedy, S. J. Olsen, R. Pebody, ECDC Public Health

Emergency Team for COVID-19, T. G. Krause, K. Mølbak, Excess all-cause mortality during the COVID-19 pandemic in Europe - preliminary pooled estimates from the EuroMOMO network, March to April 2020. *Euro Surveill.* **25** (2020), doi:10.2807/1560-7917.ES.2020.25.26.2001214.

21. M. A. Sinnathamby, H. Whitaker, L. Coughlan, J. Lopez Bernal, M. Ramsay, N. Andrews, All-cause excess mortality observed by age group and regions in the first wave of the COVID-19 pandemic in England. *Euro Surveill.* **25** (2020), doi:10.2807/1560-7917.ES.2020.25.28.2001239.

22. D. A. Leon, V. M. Shkolnikov, L. Smeeth, P. Magnus, M. Pechholdová, C. I. Jarvis, COVID-19: a need for real-time monitoring of weekly excess deaths. *Lancet*. **395**, e81 (2020).

23. UN Office for the Coordination of Humanitarian Affairs, World Health Organisation, "Syrian Arab Republic: COVID-19 Update No. 16" (2020), (available at https://reliefweb.int/report/syrian-arab-republic/syrian-arab-republic-covid-19-update-no-16-16-august-2020).

24. Syria in Context Investigation: COVID-19 Spreads out of Control in Damascus (2020), (available at https://tande.substack.com/p/syria-in-context-investigation-covid).

25. Damascus Governorate mortuary estimates 25/07/2020 - 01/08/2020. Government Organization in Damascus, Syria Facebook page (2020), (available at https://www.facebook.com/damascusgovrnorat/posts/191862302286989).

26. Statistical Abstract. 2019. Central Bureau of Statistics, Damascus-Syria, (available at http://cbssyr.sy/).

27. Interview with director of the mortuary office Firas Ibrahim by Melody FM. Who is responsible for Hawa Melody FM Facebook page (2020), (available at https://www.facebook.com/MEENALMASOOL/posts/3039607456162651).

28. Burial of the dead office: the capital cemetery can accommodate 100,000 graves. *Aliqtisadi* (2016), (available at https://aliqtisadi.com/790464-%D9%8A%D9%88%D8%AC%D8%AF-%D9%81%D9%8A-%D8%AF%D9%85%D8%B4%D9%82-%D8%B3%D8%AA-%D9%85%D9%82%D8%A7%D8%A8%D8%B1/).

29. T. Tan-Torres Edejer, O. Hanssen, A. Mirelman, P. Verboom, G. Lolong, O. J. Watson, L. L. Boulanger, A. Soucat, Projected health-care resource needs for an effective response to COVID-19 in 73 low-income and middle-income countries: a modelling study. *The Lancet Global Health* (2020), doi:10.1016/S2214-109X(20)30383-1.

30. Google, COVID-19 Community Mobility Reports, (available at https://www.google.com/covid19/mobility/).

31. #COVID19 Government Measures Dataset (2020), (available at https://www.acaps.org/covid19-government-measures-dataset).

32. H. J. T. Unwin, S. Mishra, V. C. Bradley, A. Gandy, T. A. Mellan, H. Coupland, J. Ish-Horowicz, M. A. C. Vollmer, C. Whittaker, S. L. Filippi, X. Xi, M. Monod, O. Ratmann, M. Hutchinson, F. Valka, H. Zhu, I. Hawryluk, P. Milton, K. E. C. Ainslie, M. Baguelin, A. Boonyasiri, N. F. Brazeau, L. Cattarino, Z. M. Cucunubá, G. Cuomo-Dannenburg, I. Dorigatti, O. D. Eales, J. W. Eaton, S. L. van Elsland, R. G. FitzJohn, K. A. M. Gaythorpe, W. Green, W. Hinsley, B. Jeffrey, E. Knock, D. J. Laydon, J. Lees, G.

Nedjati-Gilani, P. Nouvellet, L. C. Okell, K. V. Parag, I. Siveroni, H. A. Thompson, P. Walker, C. E. Walters, O. J. Watson, L. K. Whittles, A. Ghani, N. M. Ferguson, S. Riley, C. A. Donnelly, S. Bhatt, S. Flaxman, State-level tracking of COVID-19 in the United States. *medRxiv* (2020), , doi:10.1101/2020.07.13.20152355.

33. Syrian Ministry of Health, Syrian Arab Republic: registered cases of coronavirus, (available at https://app.powerbi.com/view?r=eyJrIjoiNTA0NWMxZmYtMDJiMC00ZWU0LTllNTktZTViZjYwYThjZmUzIiwidCI6ImY2MTBjMGI3LWJkMjQtNGIzOS04MTBiLTNkYzI4MGFmYjU5MCIsImMiOjh9&fbclid=IwAR2sdJgeMcYgezrTShcyrA3HZmqUB2_cx2PIcJguaWJQ3Rb7RRht-3EquyM).

34. M. Gharibah, Z. Mehchy, "COVID-19 pandemic: Syria's response and healthcare capacity" (The London School of Economics and Political Science, 2020), (available at http://eprints.lse.ac.uk/103841/1/CRP_covid_19_in_Syria_policy_memo_published.pdf).

35. Snapshot on WoS Health Resources and Services Availability Monitoring System (HeRAMS) 2020 Q1 : Jan- Mar - Syrian Arab Republic, (available at https://reliefweb.int/report/syrian-arab-republic/snapshot-wos-health-resources-and-services-availability-monitoring).

36. World Population Prospects - Population Division - United Nations, (available at https://population.un.org/wpp/).

37. United Nations, Department of Economic and Social Affairs, Population Division (2018). World Urbanization Prospects: The 2018 Revision, (available at https://population.un.org/wup/Country-Profiles/).

38. Syria: Weekly Report 17 – 23 July 2020 - Syrian Arab Republic. *reliefweb* (2020), (available at https://reliefweb.int/report/syrian-arab-republic/syria-weekly-report-17-23-july-2020).

39. Syria on brink of further disaster as COVID-19 cases escalate - Syrian Arab Republic. *reliefweb* (2020), (available at https://reliefweb.int/report/syrian-arab-republic/syria-brink-further-disaster-covid-19-cases-escalate).

40. R. Verity, L. C. Okell, I. Dorigatti, P. Winskill, C. Whittaker, N. Imai, G. Cuomo-Dannenburg, H. Thompson, P. G. T. Walker, H. Fu, A. Dighe, J. T. Griffin, M. Baguelin, S. Bhatia, A. Boonyasiri, A. Cori, Z. Cucunubá, R. FitzJohn, K. Gaythorpe, W. Green, A. Hamlet, W. Hinsley, D. Laydon, G. Nedjati-Gilani, S. Riley, S. van Elsland, E. Volz, H. Wang, Y. Wang, X. Xi, C. A. Donnelly, A. C. Ghani, N. M. Ferguson, Estimates of the severity of coronavirus disease 2019: a model-based analysis. *Lancet Infect. Dis.* **20**, 669–677 (2020).

41. Damascus mortality page. Facebook, (available at https://www.facebook.com/wafiatdimashq).

42. YouGov, Personal measures taken to avoid COVID-19. *YouGov* (2020), (available at https://yougov.co.uk/topics/international/articles-reports/2020/03/17/personal-measures-taken-avoid-covid-19).

43. Z. Ghosn, Why do doctors die? *https://syrianownews.com/post/2869* (2020), (available at https://syrianownews.com/post/2869).

44. UN Office for the Coordination of Humanitarian Affairs, "Syria anniversary press release (6 March 2020) - Syrian Arab Republic" (2020), (available at https://reliefweb.int/report/syrian-arab-

republic/syria-anniversary-press-release-6-march-2020).

45. T. Roberton, E. D. Carter, V. B. Chou, A. R. Stegmuller, B. D. Jackson, Y. Tam, T. Sawadogo-Lewis, N. Walker, Early estimates of the indirect effects of the COVID-19 pandemic on maternal and child mortality in low-income and middle-income countries: a modelling study. *Lancet Glob Health*. **8**, e901–e908 (2020).

46. World Health Organization. Regional Office for the Eastern Mediterranean, "HeRAMS annual report January – December 2019 public hospitals in the Syrian Arab Republic" (WHO-EM/SYR/039/E, World Health Organization. Regional Office for the Eastern Mediterranean, 2020), (available at https://apps.who.int/iris/handle/10665/333184).

47. M. U. G. Kraemer, C.-H. Yang, B. Gutierrez, C.-H. Wu, B. Klein, D. M. Pigott, Open COVID-19 Data Working Group, L. du Plessis, N. R. Faria, R. Li, W. P. Hanage, J. S. Brownstein, M. Layan, A. Vespignani, H. Tian, C. Dye, O. G. Pybus, S. V. Scarpino, The effect of human mobility and control measures on the COVID-19 epidemic in China. *Science*. **368**, 493–497 (2020).

48. Tracking Public Health and Social Measures. A Global Dataset (2020), (available at https://www.who.int/emergencies/diseases/novel-coronavirus-2019/phsm).

49. R. J. Hijmans, S. Phillips, J. Leathwick, J. Elith, dismo: Species distribution modeling. *R package version*. **1**, 1–1 (2017).

50. O. J. Watson, cwhittaker, P. Winskill, Giovanni, N. Brazeau, R. FitzJohn, patrickgtwalker, D. Hereñú, *mrc-ide/squire: v0.4.34* (2020; https://zenodo.org/record/4024244).

51. S. A. Lauer, K. H. Grantz, Q. Bi, F. K. Jones, Q. Zheng, H. R. Meredith, A. S. Azman, N. G. Reich, J. Lessler, The Incubation Period of Coronavirus Disease 2019 (COVID-19) From Publicly Reported Confirmed Cases: Estimation and Application. *Ann. Intern. Med.* **172**, 577–582 (2020).

52. Q. Bi, Y. Wu, S. Mei, C. Ye, X. Zou, Z. Zhang, X. Liu, L. Wei, S. A. Truelove, T. Zhang, W. Gao, C. Cheng, X. Tang, X. Wu, Y. Wu, B. Sun, S. Huang, Y. Sun, J. Zhang, T. Ma, J. Lessler, T. Feng, Epidemiology and transmission of COVID-19 in 391 cases and 1286 of their close contacts in Shenzhen, China: a retrospective cohort study. *Lancet Infect. Dis.* **20**, 911–919 (2020).

53. "Intensive Care National Audit & Research Centre. ICNARC report on COVID-19 in critical care, 2020."

54. Imperial College COVID-19 LMIC Reports. Version 5. MRC Centre for Global Infectious Disease Analysis, Imperial College London, (available at https://mrc-ide.github.io/global-lmic-reports/).

55. R. H. Johnstone, E. T. Y. Chang, R. Bardenet, T. P. de Boer, D. J. Gavaghan, P. Pathmanathan, R. H. Clayton, G. R. Mirams, Uncertainty and variability in models of the cardiac action potential: Can we build trustworthy models? *J. Mol. Cell. Cardiol.* **96**, 49–62 (2016).

56. Vision AI, (available at https://cloud.google.com/vision).

57. O. J. Watson, *mrc-ide/syria-covid-ascertainment: v0.1.0* (2020; https://zenodo.org/record/4030018).

58. World Health Organization (WHO) and the Office for the Coordination of Humanitarian Affairs (OCHA), Syrian Arab Republic: COVID-19 Update No. Search Results. *reliefweb*, (available at https://reliefweb.int/search/results?search=Syrian+Arab+Republic%3A+COVID-19+Update+No.).

DOI: https://doi.org/10.25561/82443

Supplementary Material

Materials and Methods

S1. Data Sources and Curation

S1.1. ACAPs Database and Inferred Mobility

We incorporate interventions using mobility data made publically available from Google (https://www.google.com/covid19/mobility/) (*30*), which provides data on movement in each country and includes the percent change in visits to places of interest (Grocery & Pharmacy, Parks, Transit Stations, Retail & Recreation, Residential, and Workplaces). We assume that mobility changes will reduce contacts outside the household, whereas the increase in residential movement will not change household contacts. Consequently, we assume that the change in transmission over time can be summarised by averaging the mobility trends for all categories except for Residential and Parks (in which we assume significant contact events are negligible). Google mobility data are unavailable for a number of countries, including Syria. For these locations, we use a Boosted Regression Tree model to infer the change in mobility over time. The model is trained using the timing and frequency of government interventions documented in the ACAPs database (*31*), with additional sources of government interventions not listed in ACAPs sourced from the WHO PHSM database (*48*), and the World Bank income status of the country. The combined intervention covariate dataset is provided in Supplementary Table 5. The model was fitted using the statistical software R and the dismo package (*49*), with tree complexity of 8, bag fraction of 0.5, and a learning rate of 0.05. 5-fold cross-validation was implemented to assess overfitting, and error associated with the test and training datasets found to be similar. The inferred mobility is then normalised such that pre-epidemic mobility is equal to 100%.

S1.2. Mortality and Incidence Data

Reported daily mortality and incidence data for Damascus was sourced from a number of sources. The majority were acquired from the Syrian Ministry of Health daily COVID-19 updates on their facebook page (https://www.facebook.com/MinistryOfHealthSYR). However, a number of historic deaths which are included in cumulative totals were not identifiable from here and were identified from the revision history of the COVID-19 pandemic in Syria Wikipedia page, which has been maintained each day by copying reported deaths and incidence data from the Syrian MoH COVID-19 dashboard (*33*), which only provides the governorate breakdown of COVID-19 for the current day.

S2. Transmission Model

To model the dynamics of a SARS-CoV-2 outbreak and its demand on healthcare over time and resultant mortality we use the same SEIR model structure as in Walker et al. (*3*). The model is parameterised to match our current best estimates of key parameters determining the natural history and spread of the virus. The model is available as an R package at https://github.com/mrc-ide/squire (Diagram 1) and is age-stratified, explicitly incorporating patterns of mixing across and between different age groups. The model includes a treatment cascade that tracks individuals with respect to their disease severity and the indicated treatment option with individuals assumed to access treatment if it is available (Diagram 2). For all analysis conducted, squire v0.4.34 was used (*50*), using the deterministic model implementation and 5 initial seeds randomly distributed in the exposed infection class.

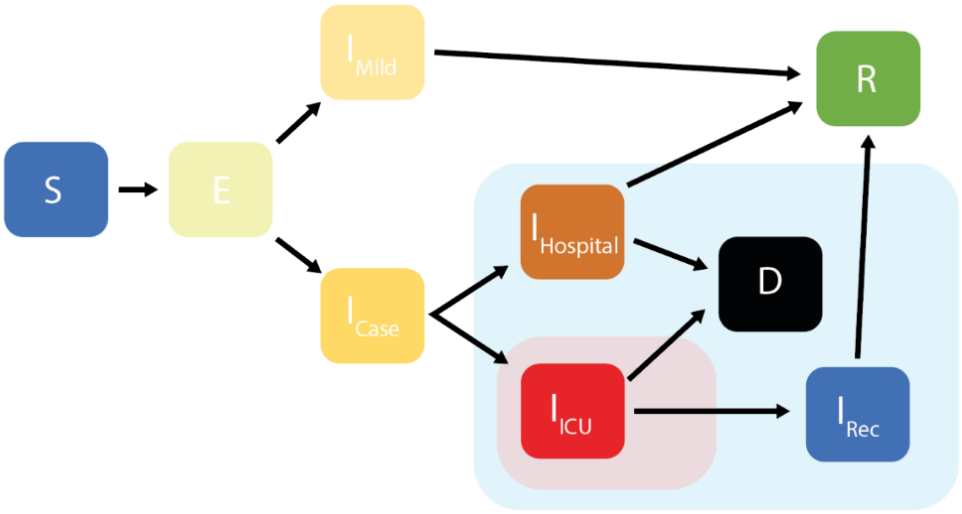

Diagram 1. Age Structured Compartmental model structure. Individuals in the population begin as susceptible to infection with SARS-CoV-2, **S**. Once infected, determined by an age-specific force of infection estimated from the age-dependent contact rates with infected individuals, and after a latent period of infection, individuals will either develop mild symptoms, I_{Mild}, or severe symptoms requiring hospitalisation, I_{Case}. Individuals in the I_{Case} compartment are then hospitalised, and will either require high pressure oxygen treatment, which will require a hospital bed, $I_{Hospital}$, or ventilator support in an ICU bed, I_{ICU}. Hospitalised cases either recover, **R**, or die, **D**. Cases in the ICU either die, **D,** or recover, **R**, after spending a period of recovery time in a hospital bed, I_{Rec}. Individuals who suffer mild symptoms, I_{Mild}, will recover after a short duration moving into the recovered compartment, **R**. The pale blue box shows compartments related to hospitalisation and occupation of general hospital beds. The pale red box shows compartments related to hospitalisations that occupy an ICU hospital bed.

DOI: https://doi.org/10.25561/82443

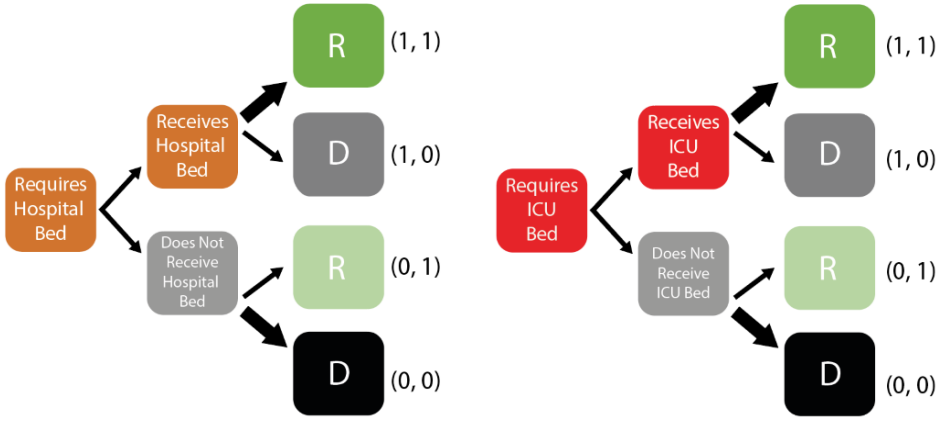

Diagram 2. Decision tree cascades to capture excess mortality with healthcare capacity being exceeded. Individuals requiring general hospital and ICU beds respectively are assigned available beds (independently of age). Those receiving a bed are subject to a lower probability of mortality than those who do not. Notation to the right hand side of each box describes the compartment in terms of the notation introduced below.

Let S(t,a) denote the susceptible population in age-group a at time t, E_1(t,a) and E_2(t,a) two sequential latent periods of infection, I_{Mild}(t,a) infections that are either asymptomatic or symptomatic but do not require hospitalisation, $I_{Case,0}$ (t,a) and $I_{Case,1}$ (t,a) two sequential states for infections that are symptomatic and will subsequently require hospitalisation. $I_{Hospital,0}$(t,a) and $I_{Hospital,1}$(t,a) are two sequential states for infections requiring a general hospital bed. $I_{ICU,0}$(t,a) and $I_{ICU,1}$(t,a) are two sequential states for infections requiring an ICU bed. $I_{REC,0}$(t,a) and $I_{REC,1}$(t,a) are two sequential states for hospitalised infections in general beds recovering from ICU whilst R(t,a) denotes those that have recovered and are immune to reinfection, and D(t,a) are those that have died from the disease in age-group a. To capture hospital capacity constraints we further split $I_{Hospital,i}$(t,a) and $I_{ICU,i}$(t,a) states (i = 1, 2) states to track those that either receive (1) or do not receive (0) their hospital or ICU bed respectively and through these route either die (0) or recover (1). These additions allow for the different durations of stay in hospital dependent on disease outcome to be captured (Diagram 2). For example, the state tracking those that require a general bed, receive it and go on to die is $I_{Hospital,i}$(t,a,1,0) whilst the state tracking those that require a general bed, do not receive it and go on to die is $I_{Hospital,i}$(t,a,0,0). In the equations below we use the Kronecker Delta function $\delta(.)$ to capture capacity constraints with this equal to 1 if there is capacity (Hospital or ICU) and zero otherwise. Contacts between age-classes are captured using the social contact mixing matrix, c(a, a'), which denotes the rate of contacts between individuals in age-groups a and a'. Age-dependent severity of disease is captured with an age-dependent mortality rate $\mu(a)$. Given that our focus is on short-term dynamics we do not model births, deaths or aging. The age-class of individuals therefore represents their age in 2020. The differential equations describing the model in full are shown below, with the parameter symbols, description and values shown in Supplementary Table 1.

DOI: https://doi.org/10.25561/82443

$$\frac{dS(t,a)}{dt} = -\beta \frac{S(t,a)}{N} \sum_{a'} c(a,a')[I_{MILD}(t,a') + I_{CASE}(t,a')]$$

$$\frac{dE_1(t,a)}{dt} = \beta \frac{S(t,a)}{N} \sum_{a'} c(a,a')[I_{MILD}(t,a') + I_{CASE}(t,a')] - 2\alpha E_1(t,a)$$

$$\frac{dE_2(t,a)}{dt} = 2\alpha E_1(t,a) - 2\alpha E_2(t,a)$$

$$\frac{dI_{MILD}(t,a)}{dt} = (1-\phi_1(a))(2\alpha E_2(t,a)) - \gamma_1 I_{MILD}(t,a)$$

$$\frac{dI_{CASE,0}(t,a)}{dt} = \phi_1(a)(2\alpha E_2(t,a)) - 2\gamma_2 I_{CASE,0}(t,a)$$

$$\frac{dI_{CASE,1}(t,a)}{dt} = 2\gamma_2 I_{CASE,0}(t,a) - 2\gamma_2 I_{CASE,1}(t,a)$$

$$\frac{dI_{HOSPITAL,0}(t,a,0,0)}{dt} = (1-\delta(H))\mu(1-\phi_2(a))2\gamma_2 I_{CASE,1}(t,a) - 2\gamma_{3,0} I_{HOSPITAL,0}(t,a,0,0)$$

$$\frac{dI_{HOSPITAL,1}(t,a,0,0)}{dt} = 2\gamma_{3,0} I_{HOSPITAL,0}(t,a,0,0) - 2\gamma_{3,0} I_{HOSPITAL,1}(t,a,0,0)$$

$$\frac{dI_{HOSPITAL,0}(t,a,1,0)}{dt} = \delta(H)\mu(1-\phi_2(a))2\gamma_2 I_{CASE,1}(t,a) - 2\gamma_{3,0} I_{HOSPITAL,0}(t,a,1,0)$$

$$\frac{dI_{HOSPITAL,1}(t,a,1,0)}{dt} = 2\gamma_{3,0} I_{HOSPITAL,0}(t,a,1,0) - 2\gamma_{3,0} I_{HOSPITAL,1}(t,a,1,0)$$

$$\frac{dI_{HOSPITAL,0}(t,a,0,1)}{dt} = (1-\delta(H))(1-\mu)(1-\phi_2(a))2\gamma_2 I_{CASE,1}(t,a) - 2\gamma_{3,0} I_{HOSPITAL,0}(t,a,0,1)$$

$$\frac{dI_{HOSPITAL,1}(t,a,0,1)}{dt} = 2\gamma_{3,0} I_{HOSPITAL,0}(t,a,0,1) - 2\gamma_{3,0} I_{HOSPITAL,1}(t,a,0,1)$$

$$\frac{dI_{HOSPITAL,0}(t,a,1,1)}{dt} = \delta(H)(1-\mu)(1-\phi_2(a))2\gamma_2 I_{CASE,1}(t,a) - 2\gamma_{3,0} I_{HOSPITAL,0}(t,a,1,1)$$

$$\frac{dI_{HOSPITAL,1}(t,a,1,1)}{dt} = 2\gamma_{3,0} I_{HOSPITAL,0}(t,a,1,1) - 2\gamma_{3,0} I_{HOSPITAL,1}(t,a,1,1)$$

$$\frac{dI_{ICU,0}(t,a,0,0)}{dt} = (1-\delta(ICU))\mu\phi_2(a)2\gamma_2 I_{CASE,1}(t,a) - 2\gamma_{4,0} I_{ICU,0}(t,a,0,0)$$

$$\frac{dI_{ICU,1}(t,a,0,0)}{dt} = 2\gamma_{4,0} I_{ICU,0}(t,a,0,0) - 2\gamma_{4,0} I_{ICU,1}(t,a,0,0)$$

$$\frac{dI_{ICU,0}(t,a,1,0)}{dt} = \delta(ICU)\mu\phi_2(a)2\gamma_2 I_{CASE,1}(t,a) - 2\gamma_{4,0} I_{ICU,0}(t,a,1,0)$$

$$\frac{dI_{ICU,1}(t,a,1,0)}{dt} = 2\gamma_{4,0} I_{ICU,0}(t,a,1,0) - 2\gamma_{4,0} I_{ICU,1}(t,a,1,0)$$

$$\frac{dI_{ICU,0}(t,a,0,1)}{dt} = (1-\delta(ICU))(1-\mu)\phi_2(a)2\gamma_2 I_{CASE,1}(t,a) - 2\gamma_{4,1} I_{ICU,0}(t,a,0,1)$$

$$\frac{dI_{ICU,1}(t,a,0,1)}{dt} = 2\gamma_{4,1} I_{ICU,0}(t,a,0,1) - 2\gamma_{4,1} I_{ICU,1}(t,a,0,1)$$

$$\frac{dI_{ICU,0}(t,a,1,1)}{dt} = \delta(ICU)(1-\mu)\phi_2(a)2\gamma_2 I_{CASE,1}(t,a) - 2\gamma_{4,1} I_{ICU,0}(t,a,1,1)$$

$$\frac{dI_{ICU,1}(t,a,1,1)}{dt} = 2\gamma_{4,1} I_{ICU,0}(t,a,1,1) - 2\gamma_{4,1} I_{ICU,1}(t,a,1,1)$$

$$\frac{dI_{REC,0}(t,a)}{dt} = 2\gamma_{4,1} I_{ICU,1}(t,a,1,1) - 2\gamma_5 I_{REC,0}(t,a)$$

$$\frac{dI_{REC,1}(t,a)}{dt} = 2\gamma_5 I_{REC,0}(t,a) - 2\gamma_5 I_{REC,1}(t,a)$$

$$\frac{dR(t,a)}{dt} = \gamma_1 I_{MILD}(t,a) + 2\gamma_{3,1} I_{HOSPITAL,1}(t,a,0,1) + 2\gamma_{3,1} I_{HOSPITAL,1}(t,a,1,1) + 2\gamma_5 I_{REC,1}(t,a) + 2\gamma_{4,1} I_{ICU,1}(t,a,0,1)$$

$$\frac{dD(t,a)}{dt} = 2\gamma_{3,0} I_{HOSPITAL,1}(t,a,0,0) + 2\gamma_{3,0} I_{HOSPITAL,1}(t,a,1,0) + 2\gamma_{4,0} I_{ICU,1}(t,a,0,0) + 2\gamma_{4,0} I_{ICU,1}(t,a,1,0)]$$

DOI: https://doi.org/10.25561/82443

Supplementary Table 1: Parameter descriptions and values.

Parameter	Symbol	Value	Description
Epidemiological Parameters			
Transmission parameter	β	-	Calculated from R_0
Basic reproduction number	R_0	-	Estimated from model fitting
Mean Latent Period	$\frac{1}{\alpha}$	4.6 days	Estimated at 5.1 days (*51*). The last 0.5 days are incorporated in the infectious periods to capture pre-symptomatic infectivity
Mean Duration of Mild Infection	$\frac{1}{\gamma_1}$	2.1 days	Incorporates 0.5 days of infectiousness prior to symptoms. In combination with mean duration of severe illness this gives a mean serial interval of 6.75 days (*52*).
Mean Duration of Severe Infection Prior to Hospitalisation	$\frac{1}{\gamma_2}$	4.5 days	Mean onset-to-admission of 4 days based on unpublished analysis of data from the ICNARC study (*53*). Includes 0.5 days of infectiousness prior to symptom onset.
Mean Duration of Hospitalisation for non-critical cases if survive	$\frac{1}{\gamma_{3,1}}$	9.5 days	Based on unpublished analysis of data from the ICNARC study (*53*).
Mean Duration of Hospitalisation for non-critical cases if die	$\frac{1}{\gamma_{3,0}}$	7.6 days	Based on unpublished analysis of data from the ICNARC study (*53*).
Mean Duration in ICU if survive	$\frac{1}{\gamma_{4,1}}$	11.3 days	Based on data from the ICNARC study (*53*) adjusted for censoring.

Mean Duration in ICU if die	$\frac{1}{\gamma_{4,0}}$	10.1 days	Based on data from the ICNARC study (*53*) adjusted for censoring.
Mean Duration in Recovery after ICU	$\frac{1}{\gamma_5}$	3.4 days	Based on unpublished analysis of data from the ICNARC study (*53*).
Probability of dying if admitted to critical care	μ	50%	Probability of death from severe infection that is treated based on data from the ICNARC study in the UK (*53*).

Age-stratified parameters			
Age adjusted IFR		0 to 4 0.003% 5 to 9 0.002% 10 to 14 0.004% 15 to 19 0.01% 20 to 24 0.02% 25 to 29 0.04% 30 to 34 0.06% 35 to 39 0.09% 40 to 44 0.13% 45 to 49 0.21% 50 to 54 0.44% 55 to 59 0.80% 60 to 64 1.68% 65 to 69 2.65% 70 to 74 4.16% 75 to 79 6.01% 80+ 9.42%	Age-stratified estimates of the IFR from Verity et al.[1]

Proportion of infections that require hospitalisation	$\phi_1(a)$	0 to 4 0.001 5 to 9 0.001 10 to 14 0.001 15 to 19 0.002 20 to 24 0.005 25 to 29 0.010 30 to 34 0.016 35 to 39 0.023 40 to 44 0.029 45 to 49 0.039 50 to 54 0.058 55 to 59 0.072 60 to 64 0.102 65 to 69 0.117 70 to 74 0.146 75 to 79 0.177 80+ 0.180	Smooth scaling age-stratified estimate of the proportion of infections that require hospitalisation from Verity et al (*40*).
Proportion of hospitalised cases requiring critical care	$\phi_2(a)$	0 to 4 0.050 5 to 9 0.050 10 to 14 0.050 15 to 19 0.050 20 to 24 0.050 25 to 29 0.050 30 to 34 0.050 35 to 39 0.053 40 to 44 0.060 45 to 49 0.075 50 to 54 0.104 55 to 59 0.149 60 to 64 0.224 65 to 69 0.307 70 to 74 0.386 75 to 79 0.461 80+ 0.709	Adjusted estimates from Verity et al (*40*).

Adjusted model parameters to capture outcomes related to poorer health outcomes and limited treatment availability			
Proportion of treated non-critical care cases dying	$\mu(a)$	0 to 4 0.25 5 to 9 0.25 10 to 14 0.25 15 to 19 0.25 20 to 24 0.25 25 to 29 0.25 30 to 34 0.25 35 to 39 0.25 40 to 44 0.25 45 to 49 0.25 50 to 54 0.25 55 to 59 0.25 60 to 64 0.25 65 to 69 0.25 70 to 74 0.25 75 to 79 0.25 80+ 0.580	Probability of death from non-severe treated infection. Values here have been adjusted to account for the potentially lower quality healthcare in a LMIC setting "poorer outcomes" in the main text. Assumed model defaults from a HIC setting are as follows: 0.013, 0.013, 0.013, 0.013, 0.013, 0.013, 0.013, 0.013, 0.015, 0.019, 0.027, 0.042, 0.069, 0.105, 0.149, 0.203, 0.580
Mean duration of hospitalisation if require critical care (ICU) but only a general bed is available		1 day	Death is likely to be quicker than in patients in high-income countries.
Probability of dying if require critical care but do not receive it	μ	95%	Probability of death from severe infection that is not treated
Probability of dying if require hospitalisation but no hospital beds and thus oxygen are available	μ	60%	We assume that the outcome is similar to not receiving oxygen.

DOI: https://doi.org/10.25561/82443

S3. Model Fitting

Using the methodological framework developed in the COVID-19 LMIC reports (*54*), we fit the daily deaths reported by the Syrian Ministry of Health for Damascus (*33*). In extension, we now explore a range of under-ascertainment values. Under-ascertainment is modelled by assuming that only a proportion of the model-predicted deaths on a given day are reported. When fitting the model, we consider the time series of deaths, D_t, as a partially-observed Markov process. We scan across a range of assumed death ascertainments to relate the Markov process to the observed realisations of death, which is given by:

$$D_t = NB(\mu.\nu, \sigma)$$

where NB is the Negative Binomial distribution, with standard deviation, σ and mean μ multiplied by the level of death under-ascertainment, ν, which is assumed to be constant throughout the epidemic. σ can be expressed as $\sqrt{\mu + \mu^2/r}$, where $r$is the dispersion parameter and assumed to be equal to 2 to account for overdispersion. The model is fit to D_t by allowing 4 parameters to vary: the start date of the epidemic, t_0, the initial R_0 in the absence of mobility changes, the effect size of mobility on transmission, M_α, and the effect size of mobility on transmission after mobility increases from its minimum, M_ω, which acts on increases in mobility relative to mobility at its minimum, $M(t_m)$. M_ω scales the impact of M_α after the minimum, such that when M_ω is equal to 1, increases in mobility after the minimum will not increase R_t, and when M_ω is equal to 0, there is no decoupling between mobility and transmission, such that R_t will increase with increasing mobility at the same rate as it decreased with decreasing mobility prior to the minimum. In addition, we include a number of pseudo-random walk parameters, ρ_i , which are introduced starting one week after the minimum in mobility, referred to as t_m, which serve to capture changes in transmission that are independent to mobility to reflect changes in human behaviour over time. The equation for the time-varying reproduction number is given by:

$$R_t = R_0 \,.\, f(-M_\alpha.(1 - M(t)) - M_\omega.M_\alpha(M(t) - M(t_m)) - \rho_1 - \rho_2 \ldots \rho_n)$$

Where $f(x) == 2\,exp(x)/(1 + exp(x))$, i.e. twice the inverse logit function, which has been used in previous models to capture the impact of mobility data on transmission (*32*). $M(t)$ is the inferred mobility throughout the epidemic, in which 1 represents 100% mobility (i.e. no change) and 0 represents 0% mobility. In order to model the changing mobility independent behaviour over time, each ρ parameter is set equal to 0 for each day prior to its start date. For example, $\rho_1$is the first mobility independent change in transmission, which starts 7 days after t_m and will be equal to 0 when $t < t_m + 7$. The estimated value for $\rho_1$is then maintained for all future time points. ρ_2 is the second mobility independent change in transmission, which starts 21 days after t_m, i.e. 2 weeks after ρ_1.The last mobility independent change in transmission, ρ_n is maintained for the last 4 weeks prior to the current day to reflect our inability to estimate the effect size of this parameter due to the approximate 21-day delay between infection and death (*3*).

Model fitting was carried within a Bayesian framework, using a Metropolis-Hastings Markov Chain Monte Carlo (MCMC) based sampling scheme, with adaptive tuning of the proposal implemented during

sampling using the Johnstone-Chang optimisation algorithm (*55*). All parameter inference results reported here are based on 10,000 iterations, 1,000 of which were discarded as burn-in. The prior distributions and ranges for each parameter estimated used are given in Supplementary Table 2. Centering the prior distribution for the effect size of mobility on transmission at 0 makes no assumption about the effect of mobility on transmission, with a value of 0 leading to R_t being invariant to changes in mobility.

Supplementary Table 2: Prior distributions and ranges

Parameter	**Distribution**	**Prior**	**Range**
R_0	Normal	Mean = 3, sd = 1	[1.6, 5.6]
Start Date	Uniform	-	60 - 10 days before first reported death
M_α	Normal	Mean = 0, sd = 3	[-10, 10]
M_ω	Uniform	-	[0, 1]
ρ_i	Normal	Mean = 0, sd = 0.2	[-5, 5]

DOI: https://doi.org/10.25561/82443

S4. Comparison to excess deaths, sensitivity analysis and model projections

We scan across a range of assumed levels of under-ascertainment of deaths between 0.05% - 20%. For each under-ascertainment value we conduct 1320 individual model fits, each one reflecting a combination of model parameters we vary as part of a sensitivity analysis testing our assumed parameters for Damascus. Full sensitivity analysis values are defined in Supplementary Table 6, but in summary we vary:

- Number of functional hospital beds.
- % of beds occupied by non-COVID-19 patients
- Effective Population Size of Damascus Governorate
- Demographic Profile of Damascus Relative to Syria
- Poorer health outcomes for patients with oxygen indicated due to insufficient oxygen supply.

From each model fit, we sample 100 parameter sets from the MCMC chain, weighted by their log likelihood. Sampled parameters are subsequently used to provide model projections. The likelihood of the model fit against the excess deaths is estimated by taking the mean log likelihood for the 100 model-predicted deaths during 25th July - 1st August compared against the government reported excess deaths during the same period. Excess deaths are similarly assumed to follow a negative binomial distribution with an expected mean value given by the model-predicted deaths, with standard deviation 2.

The best-fitting model using the default parameter set for Damascus (Supplementary Table 6) was subsequently used to provide model projections until the end of 2020. We assume that the mean mobility for the last 7 days is maintained for the remainder of 2020, yielding the final estimated R_t value to be assumed to be constant for the rest of 2020.

DOI: https://doi.org/10.25561/82443

S5. Alternative epidemic trajectories for Damascus

Due to the difficulties in only having 8-days of excess mortality data, there are multiple different epidemic trajectories that could yield the number of excess deaths reported (Supplementary Figure 6). The assumptions made so far to explore the epidemic provide just one trajectory (Supplementary Figure 6a), however, with only 8 days of excess data and a low absolute number of reported deaths it is hard to be certain that this is the correct trajectory. In Supplementary Figure 6 we identify four different scenarios through which the excess mortality could be explained:

A. Current epidemic in Damascus started in February. Due to implemented interventions, transmission remained low until restrictions were relaxed on the 26th May. After this transmission increased resulting in an epidemic. A fixed proportion of all COVID-19 deaths that occur are reported. In this scenario, the excess deaths occur before the peak of the epidemic. This is the default scenario explored in the main analysis.

B. Current epidemic in Damascus started in February. Implemented interventions were less effective than in scenario A and consequently transmission increased earlier in the year. An increasing proportion of all COVID-19 deaths that occur are assumed to be reported over time due to increased testing capacity. In this scenario, the excess deaths occur after the peak of the epidemic.

C. Current epidemic in Damascus started when interventions were relaxed on the 26th May. Due to the absence of interventions, the epidemic proceeded largely unmitigated. A fixed proportion of all COVID-19 deaths that occur are reported. In this scenario, the excess deaths occur before the peak of the epidemic.

D. The same scenario as C), except that only a fixed proportion of COVID-19 deaths that occur within hospitals are reported. Deaths that occur outside of hospitals will always be unreported. In this scenario, the excess deaths occur before the peak of the epidemic.

Each of the four scenarios would reproduce the excess deaths observed between 25th July - 1st August. However, only scenarios A) and D) would also result in both hospital capacity being reached at the end of July (in scenario B hospital capacity would have peaked prior to July) and the ascertained deaths plateauing (in scenario C ascertained deaths would continue to increase during August). For this reason, we repeated our analysis with the assumptions made in scenario D), to demonstrate that with only 8 days of excess mortality, multiple conclusions about the epidemic could be reached. Firstly, we assume that the reported COVID-19 deaths represent only a proportion of all COVID-19 deaths that occur within hospitals. Individuals who die while unable to access a hospital bed are not reported as a death. Secondly, we assume that if more than 20 days occur between reported deaths (the average time from infection to death (*3*)), then the epidemic has faded out and new infections are the result of reseeding events in Damascus.

S6. Alternative Mortality Data from Death Certificates

Due to the multiple trajectories based solely on relating the reported daily deaths to the excess deaths, we sourced an alternative source of mortality data from the "Damascus mortality" Facebook page (https://www.facebook.com/wafiatdimashq) (*41*). In Damascus, paper death certificates are affixed to household walls. These death certificates are routinely uploaded by the public to the Damascus mortality Facebook page. The last 10,000 images were available to download from the Mobile uploads and Timeline Photos album pages. Across the two sources, duplicated images were removed before identifying the local time and date at which the image was uploaded to the page. The majority of images uploaded are scans or photos of death certificates of individuals from Damascus who have recently died, however, a number of images uploaded are either images of the deceased or unrelated images. We used Google Cloud's Vision AI (*56*) to select death certificates based on being labelled as "Text" AND "Document". Where images were identified as either "Text" OR "Document", we manually inspected images to filter out non certificates, which resulted in 18 039 death certificates (Supplementary Table 7).

From the accompanying html page for each certificate, we extracted the date the image was uploaded. The file upload date is likely to have occurred after the date of death. In order to estimate the delay distribution from death to certificate upload, a random selection of 100 images were selected and translated to identify the date of death if noted on the certificate. Images were found to be uploaded within 2 days after death, with a mean delay of 0.4 days and consequently we did not adjust for a delay, with the majority of certificates uploaded on the day of death. Lastly, a small number of certificates are for individuals from Damascus (who have left the country and have relatives in Damascus) and have died outside of the governorate region (inside or outside Syria) but are uploaded to enable those in Damascus who knew the deceased to be informed about the death. Using the same subset of images used to identify the delay distribution from death to file upload, we estimated the proportion of certificates that reflect individuals who died outside of Damascus. From our subset of images, we found that 10% of individuals died outside of Damascus, with the majority dying within Rural Damascus.

In order to use death certificates to model COVID-19, we calculated a baseline certificate mortality rate, using deaths reported in 2017, 2018 and 2019. The baseline monthly mortality was estimated as 309 deaths per month, yielding a baseline of approximately 10 certificates/day. We are aware of subtle seasonal dynamics in mortality, with increased mortality during Summer and Winter. In response, we fit a negative binomial distribution to the distribution of daily deaths within each calendar month in 2017 - 2019. Using the inferred distribution, we sampled 100 estimates of the baseline certificates and subtracted this baseline from the count of daily certificates in 2020 to estimate the excess death certificates, which we assume is equal to the number of COVID-19 deaths. The resultant time series was decreased by 10% to account for deaths outside of Damascus, to yield the certificate death time series, which we used as an alternative source of data to fit the transmission model to. Lastly, the number of certificates uploaded reflects a fraction of total all-cause mortality in Damascus. 12135, 11680, 12748 deaths were reported in Damascus in 2017, 2018 and 2019 respectively (*26*). The adjusted certificate time series thus indicates that the certificates capture approximately 27.5% of total all cause mortality between 2017 - 2019. Consequently, the COVID-19 death certificate time series used is a conservative estimate of

total COVID-19 deaths. When fitting to the excess death certificates we explore a range of assumptions about the assumed fraction of total COVID-19 deaths that are captured by the excess certificate deaths. These include the 27.5% estimate based on total historic deaths and 100%, which together provide a lower and upper bound for the analysis. Lastly, we derive a central estimate by fitting to the government reported 8-day excess mortality.

S7. Data and Code Availability

All software code, data, supplementary tables, analysis scripts and figures are available in an R research compendium at https://github.com/mrc-ide/syria-covid-ascertainment (*57*).

DOI: https://doi.org/10.25561/82443

S8. Supplementary Figures

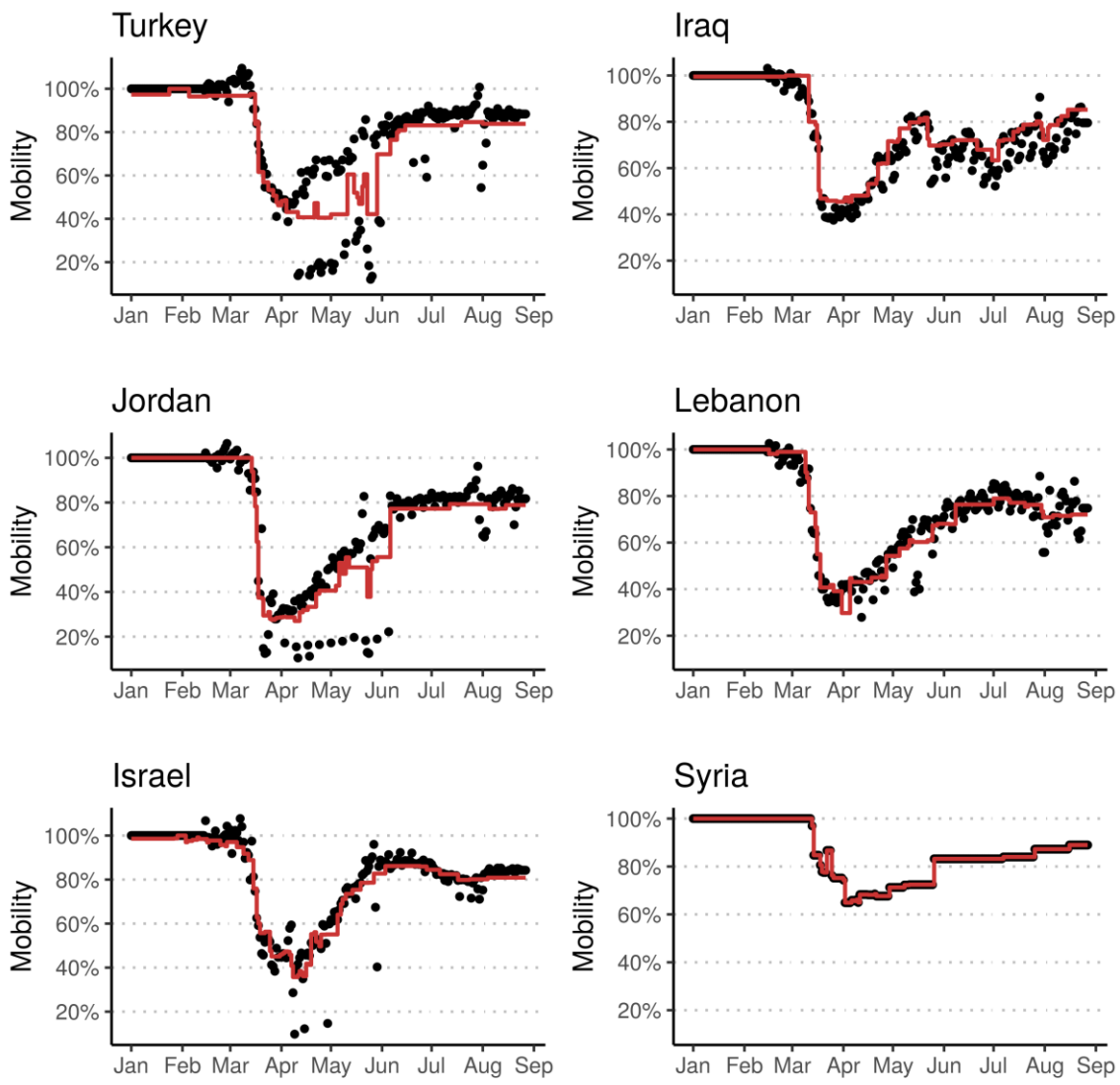

Supplementary Figure 1. Performance of Boosted Regression Tree model for predicting mobility in the Middle East. The points in each plot show the observed national mobility from the Google Mobility Reports. The red line shows the prediction of the Boosted Regression Tree model that infers mobility based on government interventions reported in the ACAPs database. For each country shown, apart from Syria, the true mobility profile is known.

DOI: https://doi.org/10.25561/82443

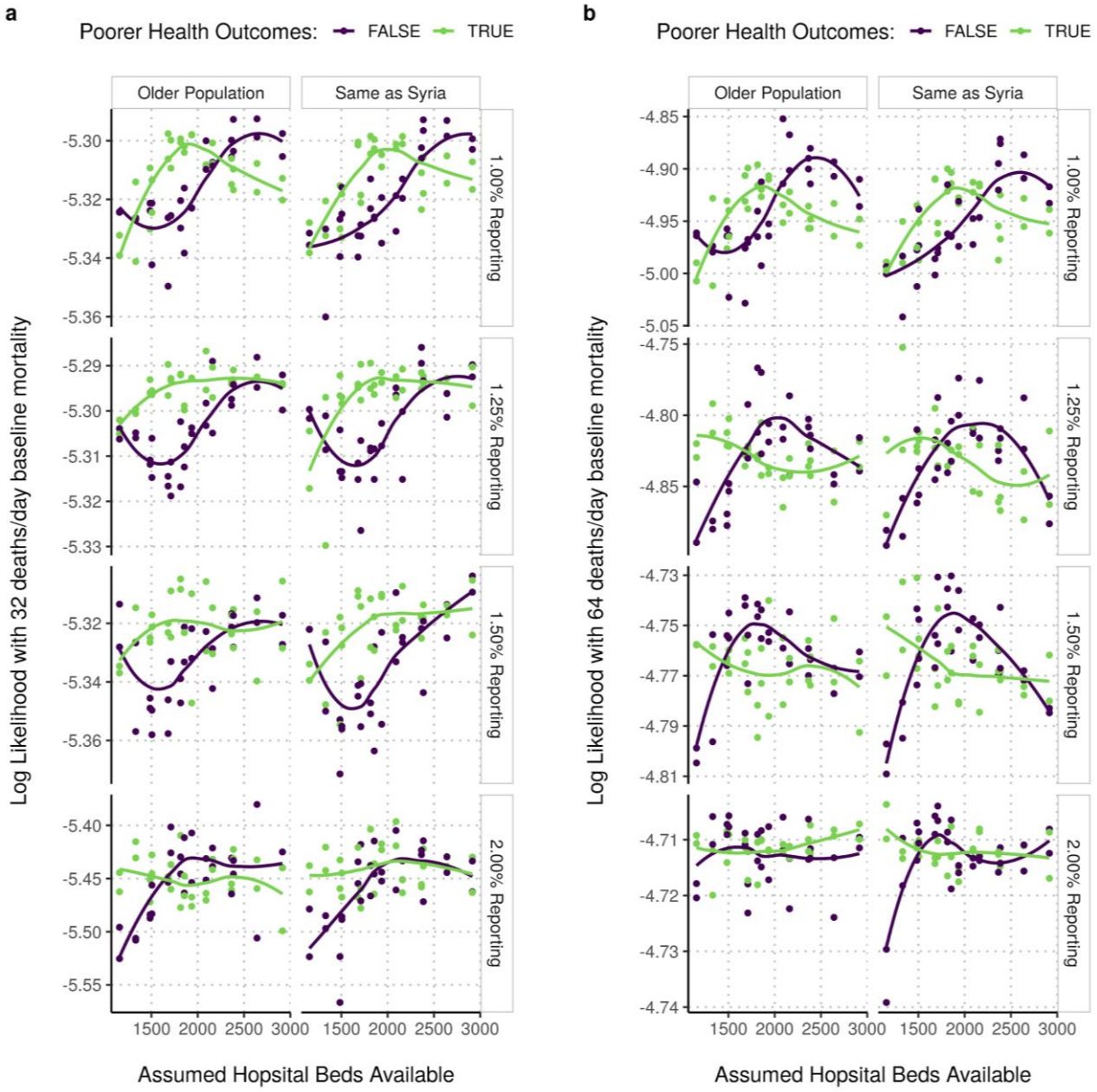

Supplementary Figure 2. Sensitivity analysis of under-ascertainment of deaths. The log likelihood of each model fit is shown, estimated by comparison to excess mortality between 25th July - 1st August 2020, with two baseline mortalities shown in a) and b). The assumed number of beds available after accounting for non-COVID-19 bed demand is shown on the x-axis, with the impact of the assumed health outcomes shown in purple and green. Lastly, the likelihoods shown are subset by the assumed demographic profile used (Older Population compared to Syria or the Same). Model likelihoods are only shown for ascertainment fractions between 1% - 2%, which were identified as being the most likely maximum range for under-ascertainment in Figure 1b for the default parameters. Each point shows a different assumed population size for Damascus governorate.

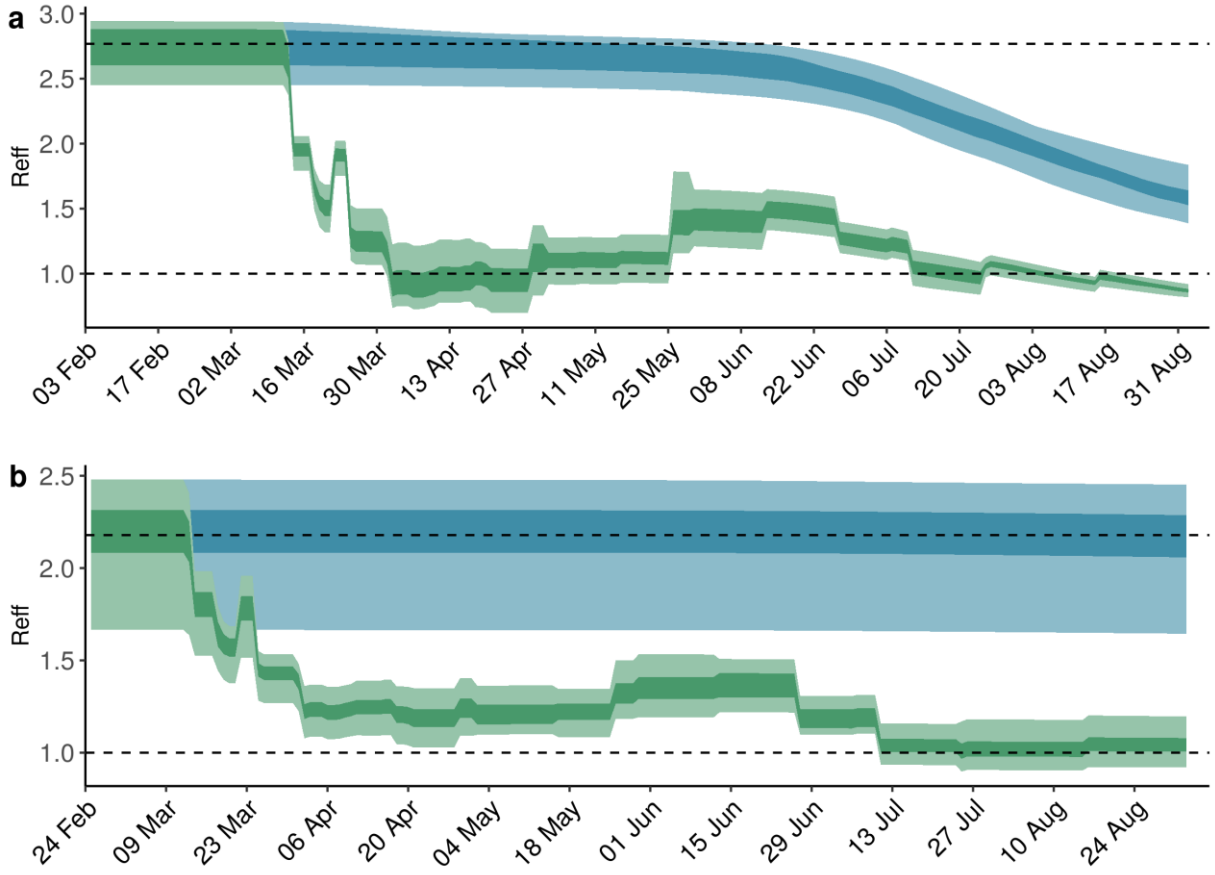

Supplementary Figure 3. Time-varying effective reproduction number, R_{eff}, for Damascus. R_{eff} (green) is the average number of secondary infections caused by a single infected person at time equal to t. A horizontal dashed line is shown at $R_{eff} = 1$. $R_{eff} < 1$ indicates a slowing epidemic in which new infections are not increasing. $R_{eff} > 1$ indicates a growing epidemic in which new infections are increasing over time. Dark green shows the 50% CI and light green shows the 95% CI. The curve in blue shows the predicted decrease in R_{eff} due to increasing immunity in the population resulting from people being infected by COVID-19. Dark blue shows the 50% CI and light blue shows the 95% CI. Individuals infected with COVID-19 are assumed to remain immune within our analysis. In a) the estimated R_{eff} is shown for Damascus with 1.25% under-ascertainment and default parameters and in b) the estimated R_{eff} is shown for Damascus assuming 100% reporting of deaths. The upper horizontal dashed line shows the value of R_{eff} at the beginning of the epidemic, which is equal to the basic reproduction number R_0, highlighting the recent role of immunity in shaping transmission in Damascus in a). Under the assumption of perfect reporting of deaths in b), decreases in transmission will have had to have occurred during a period that occurs just after the majority of interventions were relaxed in Damascus, suggesting under-ascertainment of deaths is a more parsimonious explanation.

DOI: https://doi.org/10.25561/82443

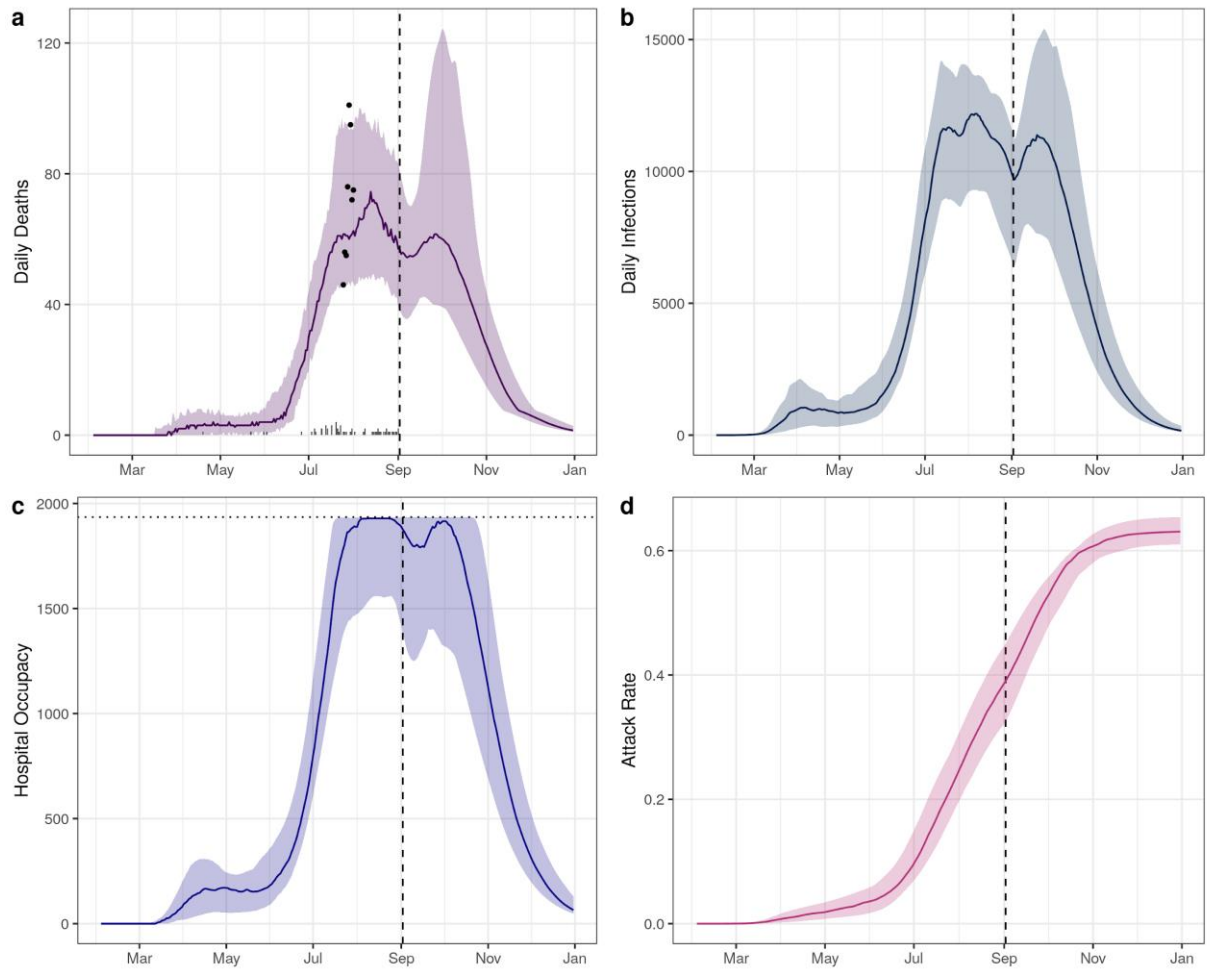

Supplementary Figure 4. Model-predicted infections, deaths, hospital occupancy and attack rates of COVID-19 for Damascus if interventions are relaxed. The predicted trajectory for the epidemic if interventions are relaxed, leading to R_t increasing from 1.48 to 2. In a) and b) the reported daily deaths and infections due to COVID-19 respectively are shown, with the estimated excess deaths for a baseline mortality of 32 deaths per day shown in a) as points. In c) hospital occupancy over time is shown, with the dotted horizontal line showing the hospital capacity available. In d) the attack rate in Damascus is shown. In all plots, the confidence interval represents the 95% quantile range and a vertical dashed line is shown for 2nd September 2020 when the analysis was conducted.

DOI: https://doi.org/10.25561/82443

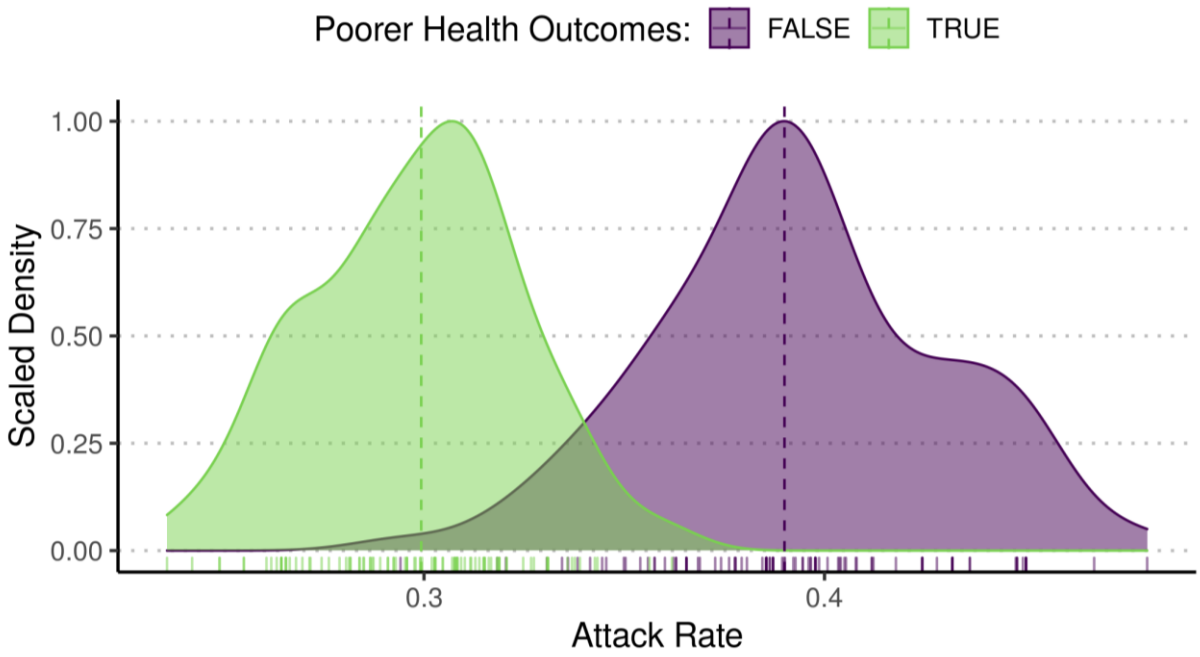

Supplementary Figure 5. Impact of assumed health outcomes on the attack rate by 2nd September 2020. The scaled density of sampled attack rates by 2nd September 2020 is shown for Damascus with 1.25% deaths reported. When poorer health outcomes compared to estimates in Verity et al. are assumed, a lower overall attack rate is observed with an 0.09 absolute increase in median attack rate.

DOI: https://doi.org/10.25561/82443

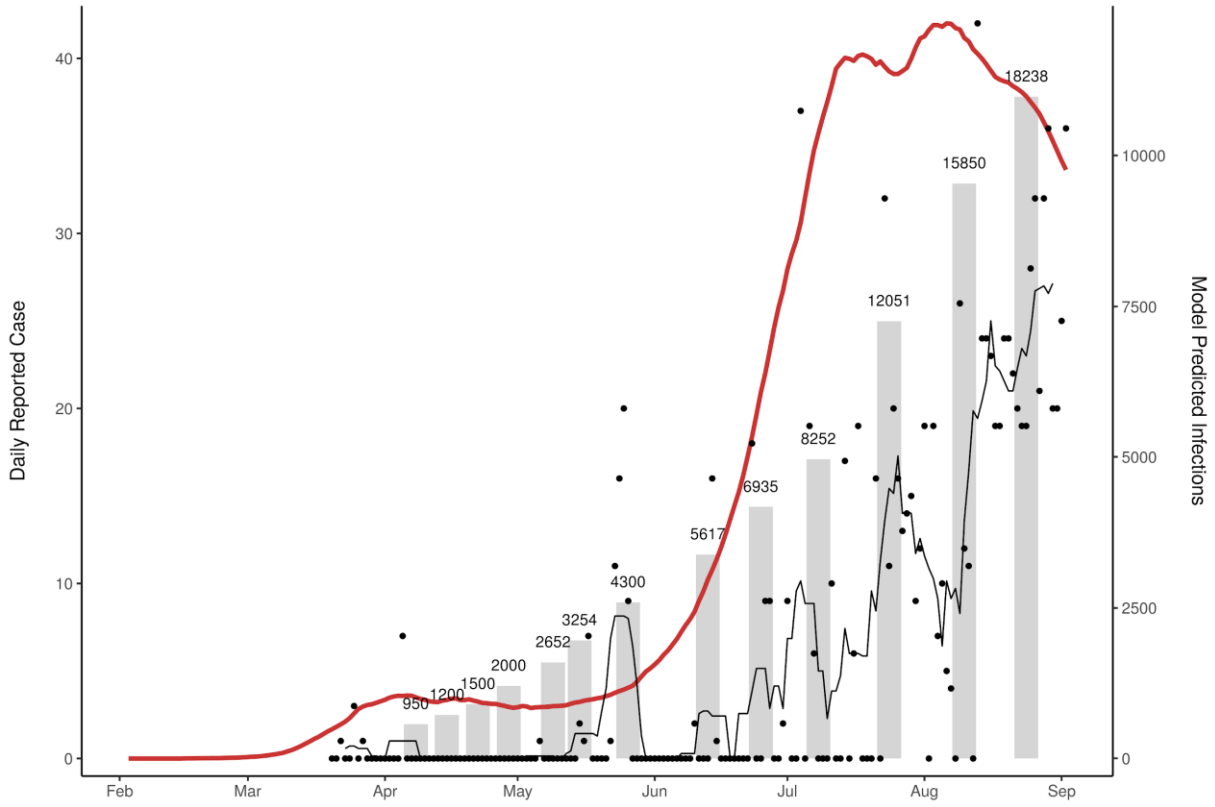

Supplementary Figure 6. Incidence of COVID-19 in Damascus and scale up of testing. Daily reported cases in Damascus are shown with points and the seven-day rolling mean incidence with the black line. The cumulative number of tests reported in Damascus from World Health Organization (WHO) and the Office for the Coordination of Humanitarian Affairs (OCHA) COVID-19 situation updates (*58*) are shown with vertical grey bars. The model-predicted incidence of infections, including asymptomatic and symptomatic infections, is shown in red.

DOI: https://doi.org/10.25561/82443

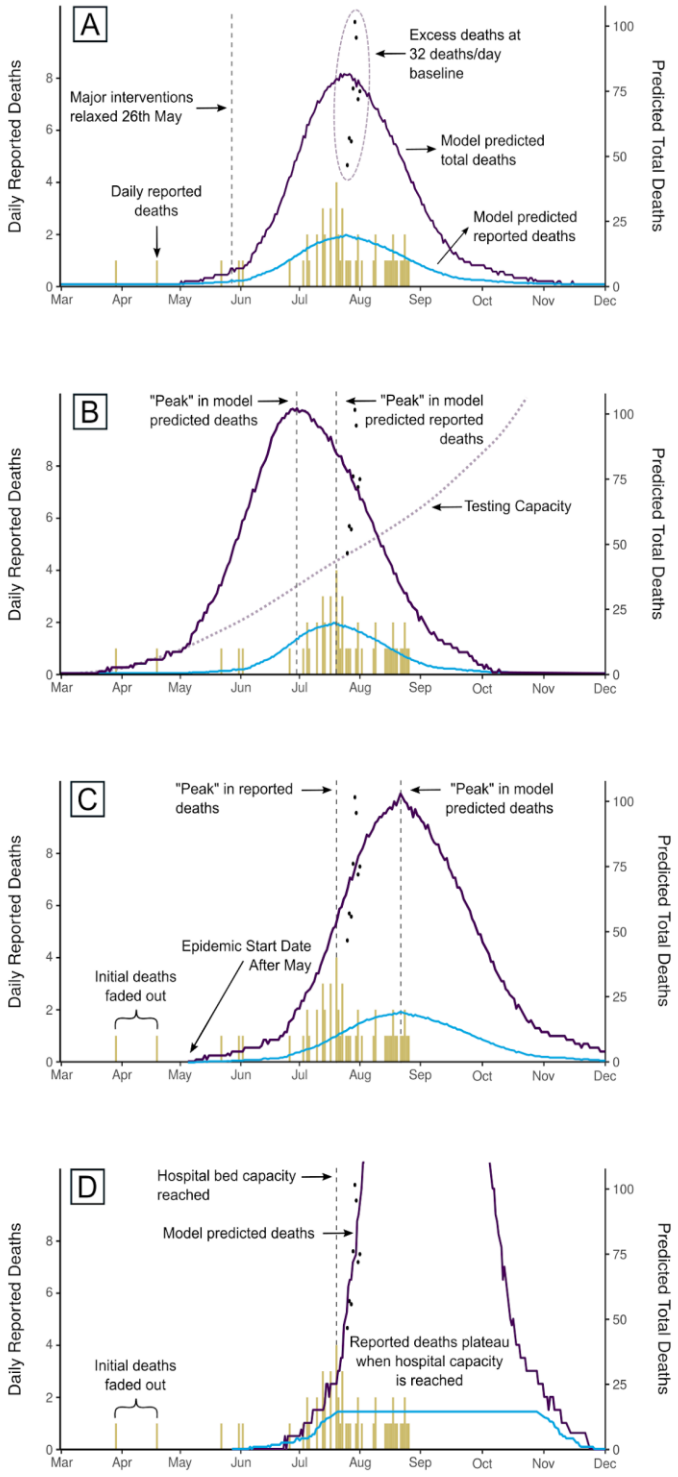

Supplementary Figure 7. Alternative epidemic trajectories. There are multiple epidemics that would reproduce the reported excess mortality. Our default assumptions yield the trajectory shown in A), with transmission remaining low from March onwards until interventions were relaxed leading to an increase in model-predicted deaths (purple), which given high under-ascertainment results in the model-predicted reported deaths (blue) fitting the reported deaths (gold bars) well. In B), the trajectory passes through the excess deaths after the peak in deaths occurred weeks earlier. However, the scale up in testing capacity, the model-predicted reported deaths still fit the reported deaths well. However, this trajectory would suggest hospital capacity would have been exceeded in June, which does not agree with reported capacity. In C), we assume the initial deaths in March and April stochastically faded out, and the epidemic observed is due to recent importation into Damascus. This results in the trajectory passing through excess deaths before reaching its peak. However, this would result in the peak of model-predicted reported deaths occurring weeks after the observed peak in reported deaths. In D), we assume that deaths can only be reported from individuals who access healthcare and thus will flatten after healthcare capacity is reached. This assumption would both fit the observed reported deaths, while also capturing the timing of healthcare capacity being exceeded and reproducing the excess deaths well.

DOI: https://doi.org/10.25561/82443

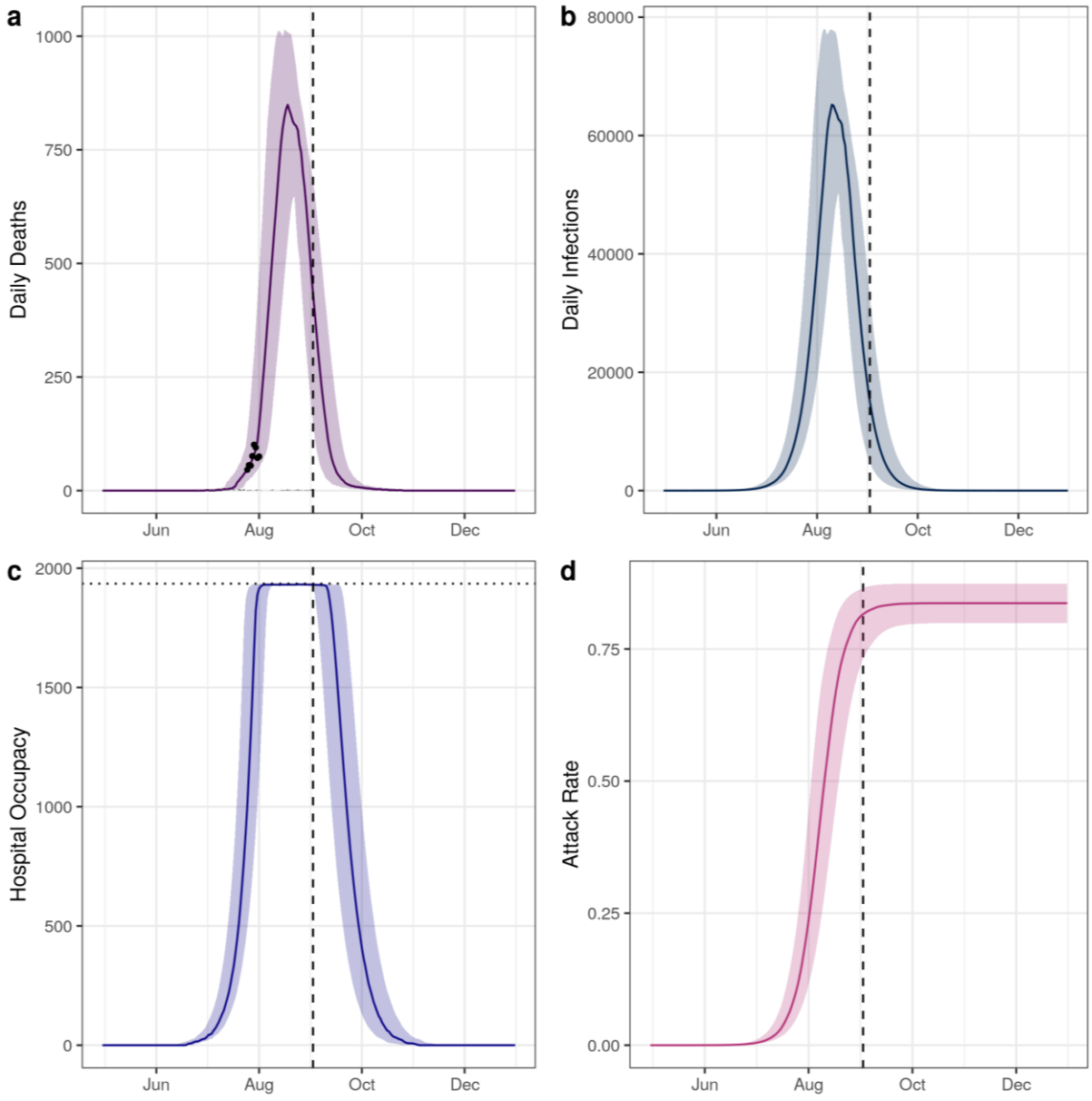

Supplementary Figure 8. Model-predicted deaths, infections, hospital occupancy and attack rates of COVID-19 for Damascus under the assumption that deaths are only ascertained from individuals who access treatment. In a) and b) the reported daily deaths and infections due to COVID-19 respectively are shown, with the estimated excess deaths for a baseline mortality of 32 deaths per day shown in a) as points. In c) hospital occupancy over time is shown, with the dotted horizontal line showing the hospital capacity available. In d) the attack rate in Damascus is shown. In all plots, the confidence interval represents the 95% quantile range and a vertical dashed line is shown for 2nd September 2020 when the analysis was conducted.

DOI: https://doi.org/10.25561/82443

S9. Supplementary Tables

Supplementary Table 3: Reported all cause mortality in Damascus governorate between 25th July - 1st August 2020 (*25*).

Date	Deaths
2020-07-25	78
2020-07-26	88
2020-07-27	87
2020-07-28	108
2020-07-29	133
2020-07-30	127
2020-07-31	104
2020-08-01	107

Supplementary Table 4: Daily Reported Deaths in Syria by governorate (*33*)**.** Table is attached as separate document (supp_table_4.csv)

Supplementary Table 5: Government COVID-19 Intervention Policy data. Date and style of government intervention policy is sourced primarily from the acaps government measures dataset (*31*) with missing policies sourced from the WHO public health and social measures (PHSMs) database (*48*). Table is attached as separate document (supp_table_5.csv)

DOI: https://doi.org/10.25561/82443

Supplementary Table 6: Sensitivity Analysis Details. All combinations of parameters below were explored leading to 1,320 different model fits conducted. The default parameter values are shown in bold, with % of Deaths ascertained not having any value in bold as this was the investigated parameter we were scanning across.

Description	**Values**
% of Deaths Ascertained	20.00%, 10.00%, 6.00%, 3.00%, 2.00%, 1.50%, 1.25%, 1.00%, 0.50%, 0.10%, 0.05%
Number of functional hospital beds	3 300, 3 800, **4 300**, 4 800, 5 800
% of beds occupied by non-COVID-19 patients	45%, **55%,** 65%
Population Size of Damascus Governorate	**2 392 000**, 4 800 000
Demographic Profile of Damascus Relative to Syria	**Same Age**, Older Population
Poorer health outcomes for patients with oxygen indicated due to insufficient oxygen supply.	**False** (IFR same as Verity et al (*40*)), True (Increased probability of death from individuals with oxygen indicated who receive oxygen as introduced in Walker et al. (*3*))
Deaths Prior to 26th June led to epidemic fade outs and epidemic observed in July and August due to reseeding events.	**False**, True (Explored in Alternative Epidemic Trajectories Analysis)

Supplementary Table 7: Facebook death certificate data. Death certificates were processed using Google's Vision AI API to filter out images that were not death certificates. Details of the image labelling are shown. Certificates that were labelled as both "text" and "document" were identified as certificates. Images labelled as only one of "text" and "document" were manually checked and marked to not be included if the image was not a certificate. Table is attached as separate document (supp_table_7.csv)

DOI: https://doi.org/10.25561/82443